

MATERIALS AND METHODS:

Long-lived protein degradation assay. Long-lived protein assay was done according to the published protocol (Pattingre et al. 2004). Cells are labeled for 18 hours at 37 °C with 0.2 mCi/ml of $-[^{14}\text{C}]$ valine in complete medium DMEM (GIBCO), 10% fetal bovine serum (Hyclone), 1% penicillin–streptomycin. Unincorporated radioactivity is removed by three times rinse with PBS. Cells are then incubated in Hanks' balanced salt solution (HBSS, GIBCO), plus 0.1% of bovine serum albumin (BSA), and 10 mM valine (Sigma) to stimulate autophagy. When required, 10 mM 3-MA (3-methyladenine; Sigma) is added throughout the chase period to inhibit the formation of autophagic vacuoles. After the first hour of incubation, at which time short-lived proteins are being degraded, the medium is replaced with the fresh medium, and incubation is continued for an additional 4 hours period. Thereafter, the medium is precipitated with trichloroacetic acid (TCA) added to a final 10% concentration. After centrifugation for 10 min at 2000 rpm at 4 °C, the acid-soluble radioactivity is measured by liquid scintillation counting. Cells are washed twice with cold 10% TCA and dissolved at 37°C in 0.2 N NaOH. Radioactivity is then measured by liquid scintillation counting. The rate of long-lived protein degradation is calculated from the ratio of the acid-soluble radioactivity in the medium to the cell acid precipitable fraction.

In vitro fusion assay. Autophagosomes, autophagolysosomes and lysosomes were isolated from cultured cells using a protocol that was modified from previous reference (Marzella et al. 1982). Briefly, cells were lysed by nitrogen cavitation and a pellet enriched in autophagic and lysosomal components and in mitochondria was prepared by differential centrifugation. The different components of this pellet were separated by

centrifugation in a discontinuous metrizamide gradient as described before (Yu et al. 2005). Fractions were collected from the interfaces of the gradient, washed by centrifugation in 0.25M sucrose and resuspended in 10mM MOPS pH 7.2/0.25M sucrose. Autophagosomes were labeled by sequential 5 min incubations at room temperature with an antibody against LC3 and an FITC-conjugated secondary antibody. The lysosomes in the lysosomal-enriched fraction were labeled in a similar manner but with a primary antibody against LAMP-2 and a Cy5-conjugated secondary antibody. Labeled fractions were washed and resuspended in fusion buffer (10 mM HEPES pH 7, 10 mM KCl, 1.5mM MgCl₂, 1mM DTT in 0.25M Sucrose). Labeled fractions were mixed and supplemented with 2mM CaCl₂, 2mM GTP, 3mM ATP and an energy regenerating system (8mM Phosphocreatine and 0.16mg/ml creatine phosphokinase). After 30 min incubation at 37 C, the reaction was spotted in a coverslip and stopped by fixation with 8% formaldehyde in 0.25M sucrose for 15 min on ice. After addition of mounting media images of the slides were acquired with an Axiovert 200 fluorescence microscope (Carl Zeiss Ltd., Thornwood, NY). Quantification was performed using Image J software (NIH, MD) with the JACoP plug-in. At least 3 different experiments and 4-6 different fields per condition and experiment were imaged and quantified (average total number of particles was approximately 800-1200 particles). Fluorescence structures >4 diameters above the average particle diameter were eliminated from the counting as they were probably “vesicular” clumps impossible to completely eliminate from the preparation without affecting the stability of the other vesicle membranes. Fusion events were quantified as the percentage of vesicles positive for both fluorophores. Mean values of the 8 different fields were used to calculate the mean value of the different experiments.

The protocol for the isolation and labeling of autophagosomes and lysosomes from livers of fed or 6 hour starved mice was identical but homogenization was used instead to disrupt the hepatocytes. In this case, lysosomes were isolated from wild type mice and labeled as above, whereas autophagosomes were isolated from GFP-LC3 mice to avoid need of further labeling of that fraction. Where indicated, autophagosomes and/or lysosomes were treated with 200 μ M lantrunculin A for 20 min at 25°C and recovered by centrifugation before adding them to the fusion reaction. Rabbit skeletal muscle actin (20 μ g/ml) was added in some reactions during fusion.

Immunogold staining. Immunogold labeling was performed in cells fixed in 4% paraformaldehyde/0.1% gluteraldehyde in 0.1M cacodylate buffer. Briefly, cellular monolayers were for 1 h at room temperature, dehydrated, embedded in Lowicryl and cut in ultrathin sections. Each grid was washed in 50 mM glycine in phosphate buffered saline, blocked and preincubated in the antibody incubation buffer for 1 h. Blocked grids were incubated with the antibody against LC3 for 2 h, extensively washed and incubated with the gold-conjugated secondary antibody (1:100) for another 2 h. Control grids were incubated with either an irrelevant IgG and the secondary antibody under the same conditions or only with the secondary antibody. After extensive washing, samples were fixed a second time for 5 min in 2% gluteraldehyde washed and negatively stained with 1% uranyl acetate for 15 min. All grids were viewed on a JEOL 100CX II transmission electron microscope at 80 kV

Histology and immunohistochemistry of *Drosophila* eye sections. Fly heads of the appropriate genotype were collected and fixed in 4% paraformaldehyde in phosphate buffered saline (PBS) for 2 hours at room temperature or overnight at 4 °C. The samples

were then dehydrated using a series of one hour ethanol incubations (50 %, 70 %, 80 %, 90 %, 95 %, and twice at 100 %). Following dehydration, samples were infiltrated by JB-4 infiltration solution (JB-4 plus solution A and benzoyl peroxide), plasticized for 2-3 days at 4 °C, then processed to JB-4 embedding and sectioned with a microtome (LEICA model RM2255). For histological analysis, sectioned tissues were desiccated overnight at room temperature and subjected to Richardson's staining. For ubiquitin detection, sectioned tissues were blocked at 1 % BSA plus 1 % goat serum for 1 hour followed by incubation with mouse monoclonal antibody against Ubiquitin (Zymed) at 1:100 for 3-4 hours. Samples were washed with PBS three times for 5 minutes each time, and stained with an anti-mouse secondary antibody conjugated to Alexafluor 488 and DAPI (Polysciences, Inc.), cover slipped and analyzed by fluorescence microscopy.

Legend for supplemental figure.

Figure S1. LC3 antibody and mCherry-GFP-LC3 detect autophagosomes.

(A) HDAC6 KO MEFs were transfected with control and ATG5 siRNA and treated with MG132 as described in Materials and Methods and immunostained with antibodies to ubiquitin (green) and LC3 (Red). Arrows indicate ubiquitin positive protein aggregates. Scale bar, 25µm. (B) Wild type and HDAC6 KO MEFs were transfected with mCherry-GFP-LC3 and co-stained with monodansylcadaverine (MDC) to visualize autophagosomes. Yellow signals indicate non-acidic autophagosomes and red signals indicate acidic autophagolysosomes in left panel. Middle panel shows MDC staining as blue color and right panel shows merged image. Arrows indicate autophagosomes which

are labeled with mCherry-GFP-LC3 as yellow and MDC as blue. Scale bar, 10 μ m.

Figure S2. Characterization of the lysosomal system in HDAC6 knock-out cells.

(A) LysoTracker DND-99 staining of wild type (WT) and HDAC6^{-/-} MEFs (HDAC6 KO) to determine lysosomal pH. (B) Quantification of the number of LysoTracker positive puncta in the cells shown in A. (C) Immunoblots for cathepsin D of the same cells maintained in the presence or absence of serum to determine lysosomal pH through the cleavage of pro-cathepsins into their mature forms. Arrows indicate the precursor (p) and mature (m) forms of cathepsin. The percentage of cathepsin processed into mature form in each condition was calculated by densitometry. LAMP-1 is also shown. Note: the acidification of the lysosomal system is comparable in WT and HDAC6 KO MEFs.

Figure S3. Representative image of in vitro autophagosome-lysosome fusion assay.

In vitro fusion assay between autophagosomes (APG) and lysosomes (Lys) from wild type (WT) and HDAC6^{-/-} MEFs (HDAC6 KO). Arrows show the colocalization of green and red vesicles and inset panels show higher magnification images of these events. The quantification of these experiments is shown in Fig. 2C.

Figure S4. Electron microscope images for wild type MEFs under normal growth condition.

Electron microscope images of wild type MEFs in normal growth conditions. (A-B) autophagosomes and (C-I) autophagolysosomes. (J and K) low magnification images. Red letters indicate the location of the corresponding magnified image.

Figure S5. Electron microscope images for HDAC6 KO MEFs under normal growth condition.

Electron microscope images of HDAC6 KO MEFs in normal growth conditions. (**A-F**) autophagosomes and (**G-I**) autophagolysosomes. (**J** and **K**) low magnification images. Red letters indicate the location of the corresponding magnified image.

Figure S6. The vesicles that accumulate in HDAC6 knock-out cells are positive for LC3.

Immunogold labeling for LC3 of the HDAC6^{-/-} MEFs. A general area (top left) and higher magnification pictures of individual autophagic vacuoles are shown. Arrows point to gold particles associated to the inner or outer membrane of the autophagic vesicles. av (autophagic vesicles); ld (lipid droplet); lm? (Possible limiting membrane in formation).

Figure S7. HDAC6 is required for basal quality control autophagy.

(**A**) Autophagy flux was determined as increased LC3-II amount after lysosomal protease inhibition (Pepstatin A and E-64D each 10ug/ml) and are presented as mean + S.D. from 3 independent experiments. Notes: Measurement of the degradation of LC3-II under basal conditions revealed a decrease of almost 50% in the accumulation of LC3-II upon inhibition of lysosomal degradation with leupeptine, supporting thus reduced rates of delivery of this molecule to lysosomes through autophagosome/lysosome fusion. (**B**) Representative Western result for autophagy flux assay. Wild type and HDAC6 KO MEFs were incubated with normal media or HBSS with/without 20mM NH₄Cl and 100ug/ml leupeptin for 6 hours. Cell lysates were subjected to Western analysis using anti-LC3, anti-HDAC6 and anti-GAPDH antibodies. All measurements were normalized by GAPDH. (**C**) Wild type and HDAC6 KO MEFs cell lysates were subjected to Western analysis using anti-p62, anti-LC3, anti-HDAC6 and anti-GAPDH antibodies.

Figure S8. HDAC6 is also required for autophagosome-lysosome fusion under other quality control related stress.

(A) Wild type and HDAC6 KO MEFs were transfected with mCherry-GFP-LC3 and treated with Rotenone, Deferoxamine, H₂O₂, and Hank's solution for 5 hours as indicated. Yellow signals indicate non-acidic autophagosomes and red signals indicate acidic autophagolysosomes. Scale bar, 25 mm. (B) The total number of yellow vesicles was quantified from 3 independent experiments (> 10 cells each) and presented as percentage of total mCherry-GFP-LC3 dots (red plus yellow) with standard deviation.

Figure S9. HDAC6 is required for actin remodeling on ubiquitin positive aggregates.

(A) The percentage of cells with actin-surrounded aggregates in each genotype was quantified from 3 independent experiments (>100 cells per experiment, representative images are shown in Figure 4A, S1B). (B) HDAC6KO MEFs stably expressing human HDAC6WT, HDAC6CD or HDAC6 Δ BUZ mutant were treated with MG132 and stained with antibodies for ubiquitin (green), for human HDAC6 (red) and with phalloidin for actin (blue). Arrows indicate aggregates positive for F-actin.

Figure S10. Effect of actin on autophagosome/lysosome fusion in cells defective for HDAC6.

Autophagosomes (APG) and lysosomes (Lys) purified from wild type (A, C) and HDAC6^{-/-} MEFs (B, D) were treated or not with latrunculin (LatA) as indicated and subjected to *in vitro* fusion assay in the presence or absence of purified actin. MEFs were

cultured in serum (+) (**A, B**) or serum (-) (**C, D**) conditions. Values are means + S.E. of the percentages of fusion from 3 independent experiments.

Figure S11. Cortactin knockdown MEF cells are defective in aggregate clearance.

(**A**) Control and cortactin-knockdown MEFs were treated with 2.5 μ M MG132 for 24 hours, incubated in normal growth media without MG132 for 18 hours and subjected to immunocytochemistry using anti-ubiquitin antibody (green) and phalloidin (red). Arrows indicate ubiquitin aggregates. (**B**) Control and cortactin-knockdown MEFs were treated with 2.5 μ M MG132 for 18 hours. After 3 times wash with PBS, cells were incubated with full media for the indicated times. Cell lysates were subjected to Western analysis using anti-ubiquitin, anti-cortactin and anti-GAPDH antibodies. To detect ubiquitinated protein aggregates, the stacking gel was transferred and blotted with anti-ubiquitin antibody.

Figure S12. Basal autophagosomes contains ubiquitinated proteins.

Purified autophagosome and lysosome fractions from wild type MEFs under normal growth media or serum starvation were subjected to immunoblot for ubiquitin. Ubiquitinated protein aggregates are detected in the base of the wells visible upon transferring of the stacking gel.. cytosol (cyt); Autophagosomes (APGs); lysosomes

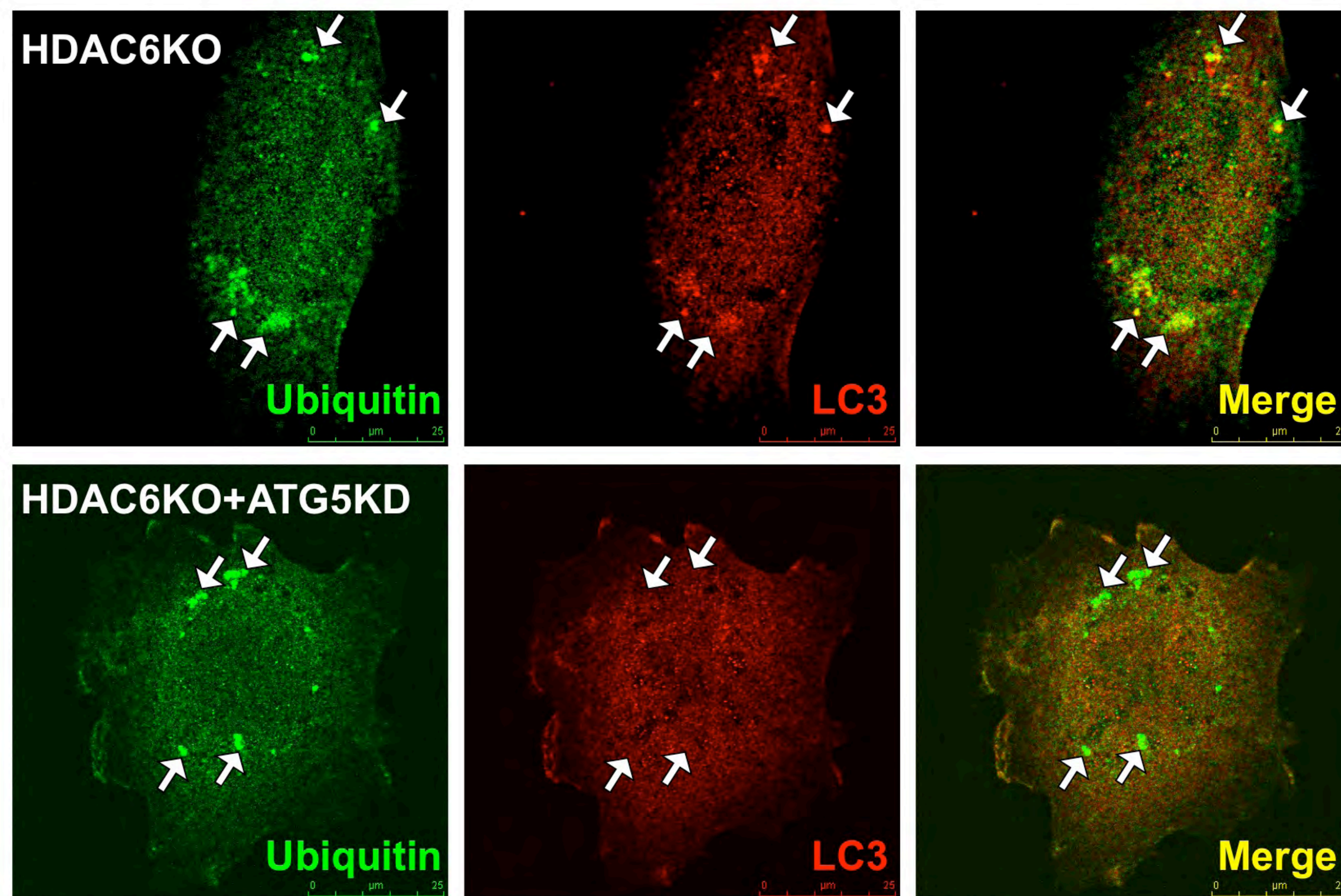
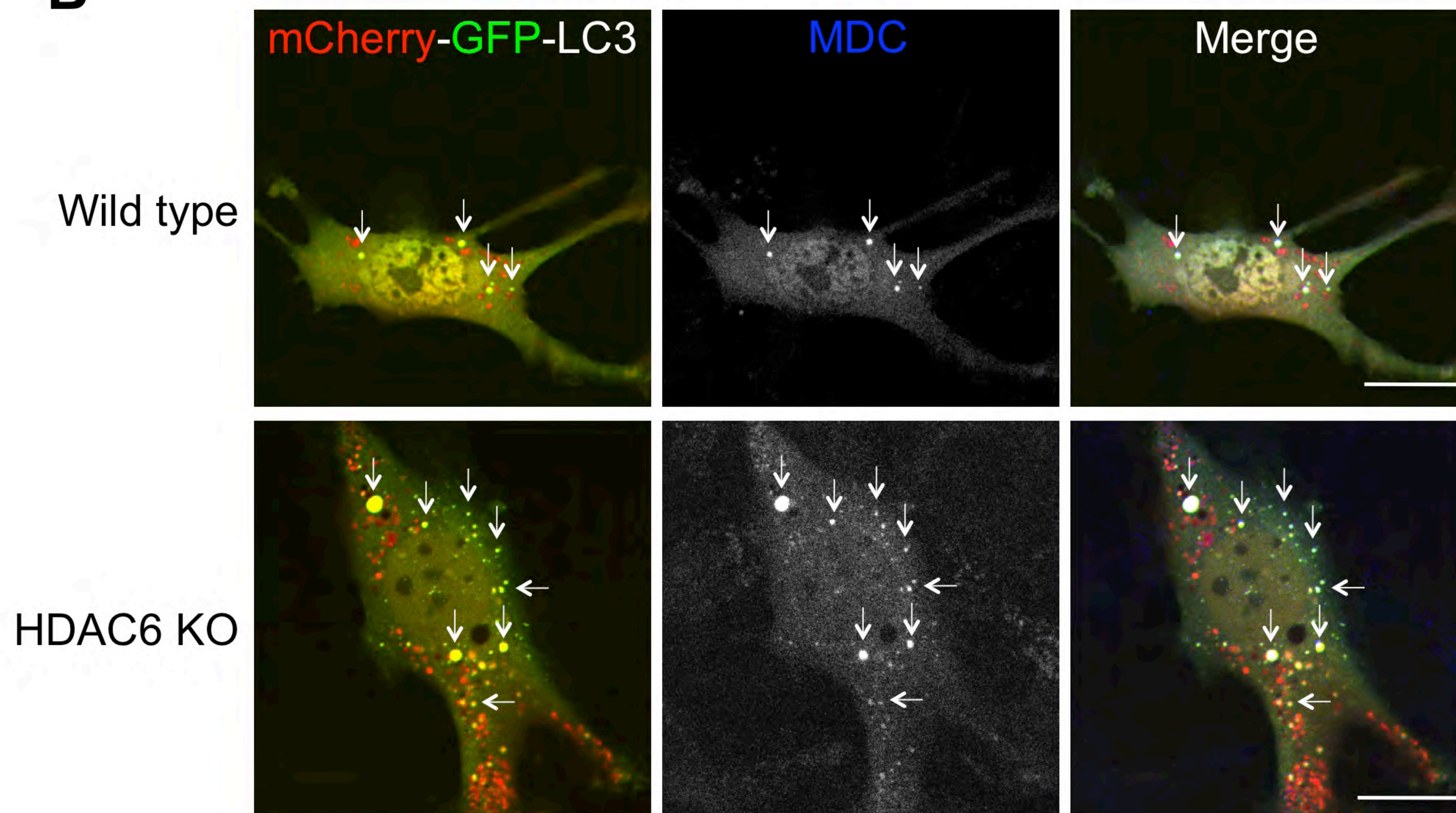
Figure S13. A model for HDAC6-dependent clearance of ubiquitinated protein aggregates by autophagy.

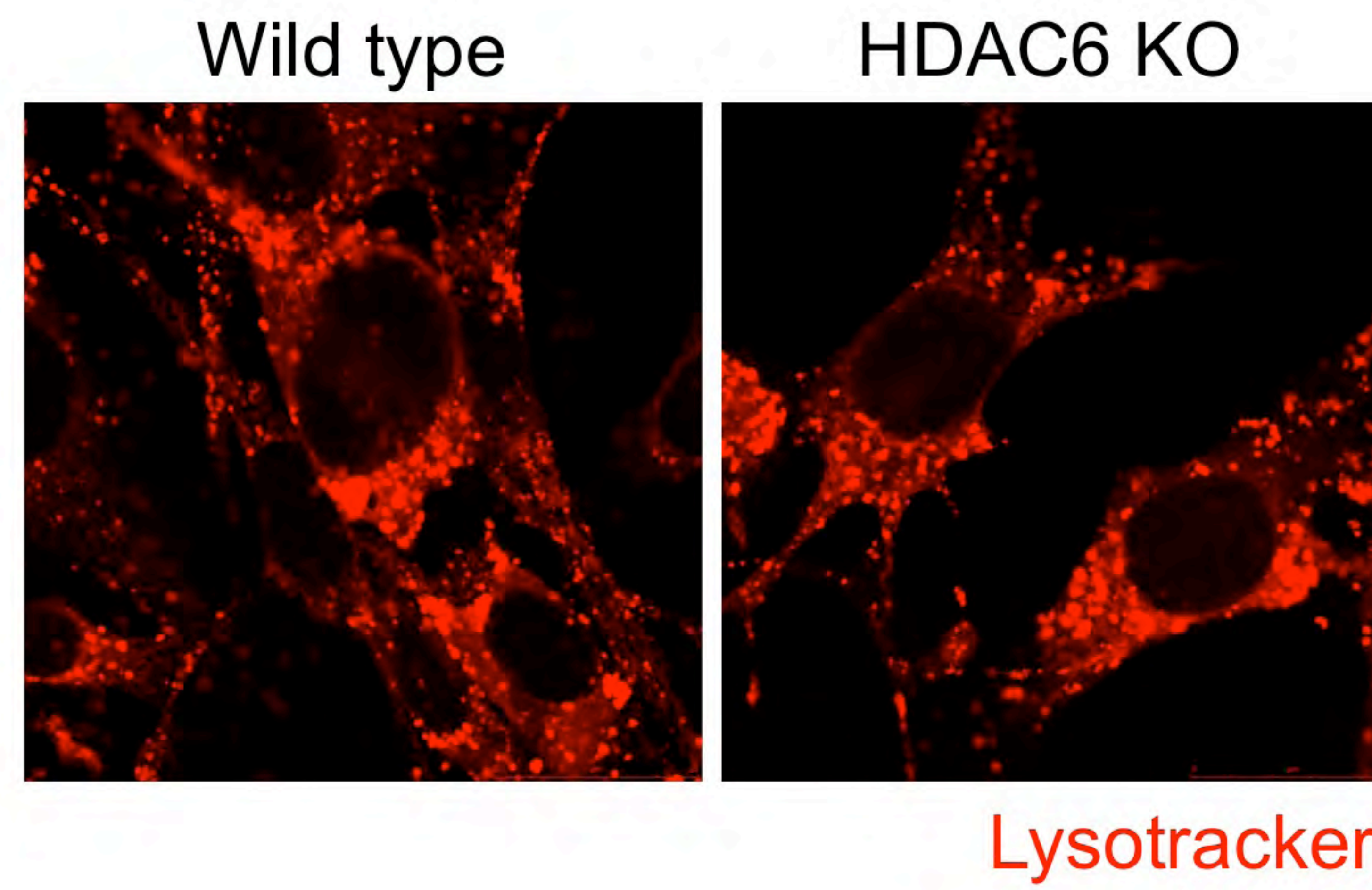
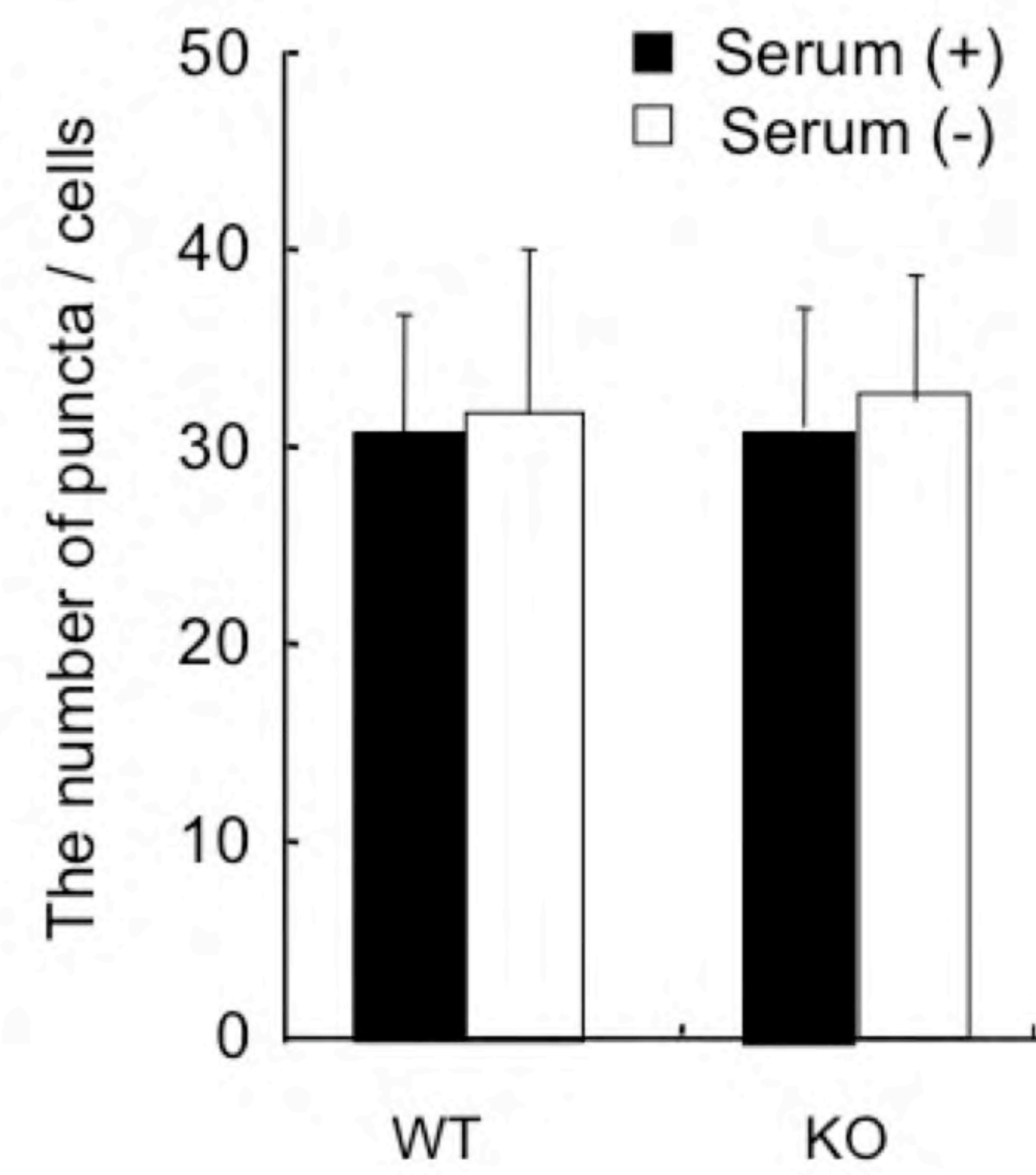
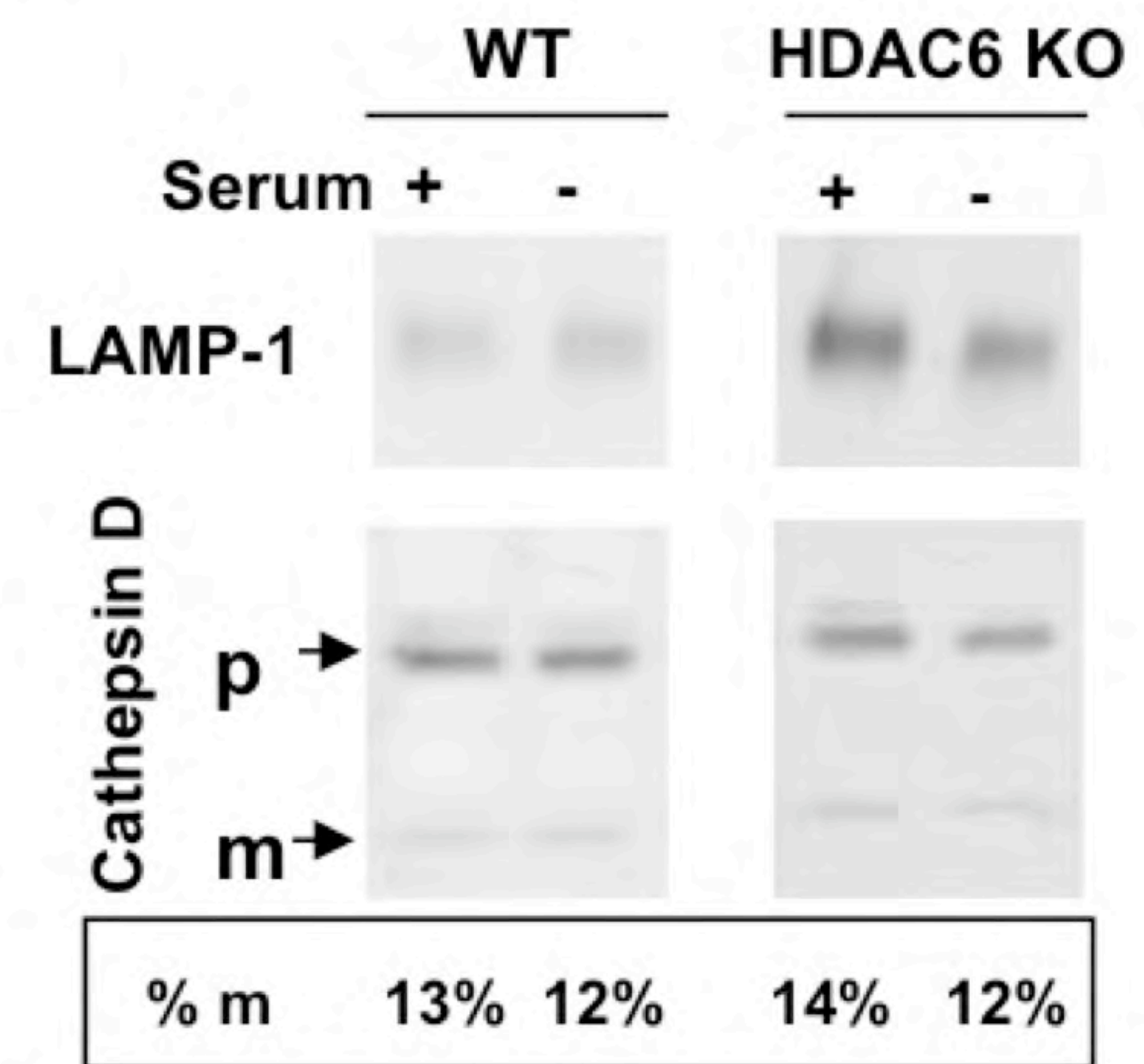
Our findings indicate that HDAC6 could promote protein aggregate clearance at multiple levels. HDAC6 facilitates the transport of ubiquitinated protein aggregates to form aggresomes via the microtubule network (Kawaguchi et al. 2003) and enhances their

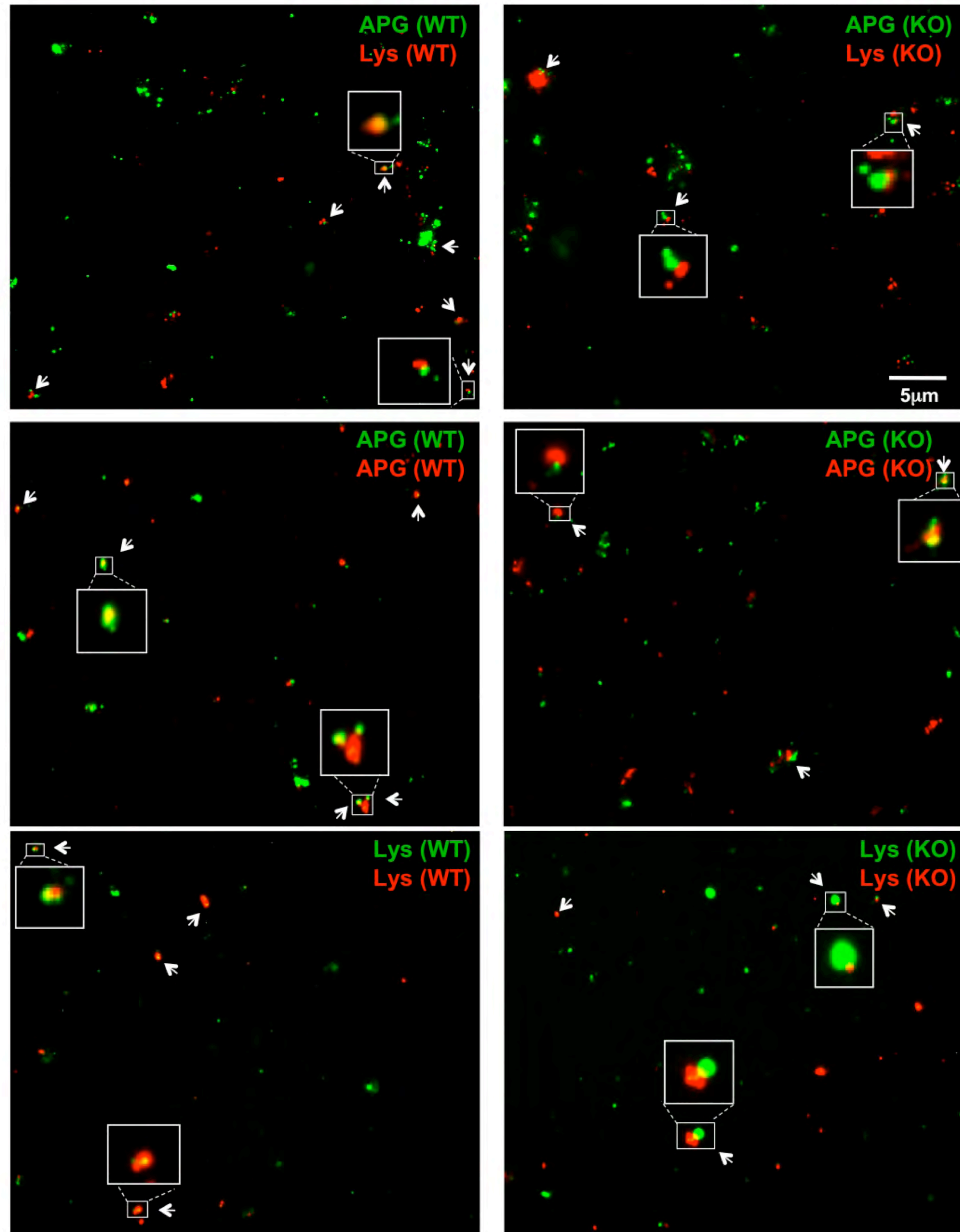
subsequent clearance by stimulating the fusion of autophagosomes and lysosomes via the actin network. It is certainly conceivable that HDAC6 could further promote this process by regulating the dynein motor-dependent transport of lysosomes to protein aggregates (Iwata et al. 2005). Thus, HDAC6 would function as a key factor in basal homeostatic autophagy by coordinating both the transport of autophagic components and eventual fusion events via its unique association with the microtubule and actin cytoskeleton. (1) The protein aggregates are first independently recognized and bound by HDAC6 and p62 through the presence of specific polyubiquitin chains. The bound HDAC6 recruits cortactin to protein aggregates (2) and deacetylates cortactin to generate an actin network (3), which retains and concentrates lysosomes surrounding aggregates. The initial transport of lysosomes to aggregates could involve microtubules (MT). (2) The aggregate-bound p62 would independently recruit LC3 and the formation of autophagosomes that sequester oligomeric or small protein aggregates. (4) The actin network further promotes the fusion of autophagosomes and lysosomes, (5) leading to the eventual degradation of the protein aggregates. Under pathological conditions when excessive protein aggregates accumulate, the autophagy efficiency could be further enhanced by the HDAC6-dependent transport of aggregates and lysosomes to the MTOC (Microtubule Organizing Center).

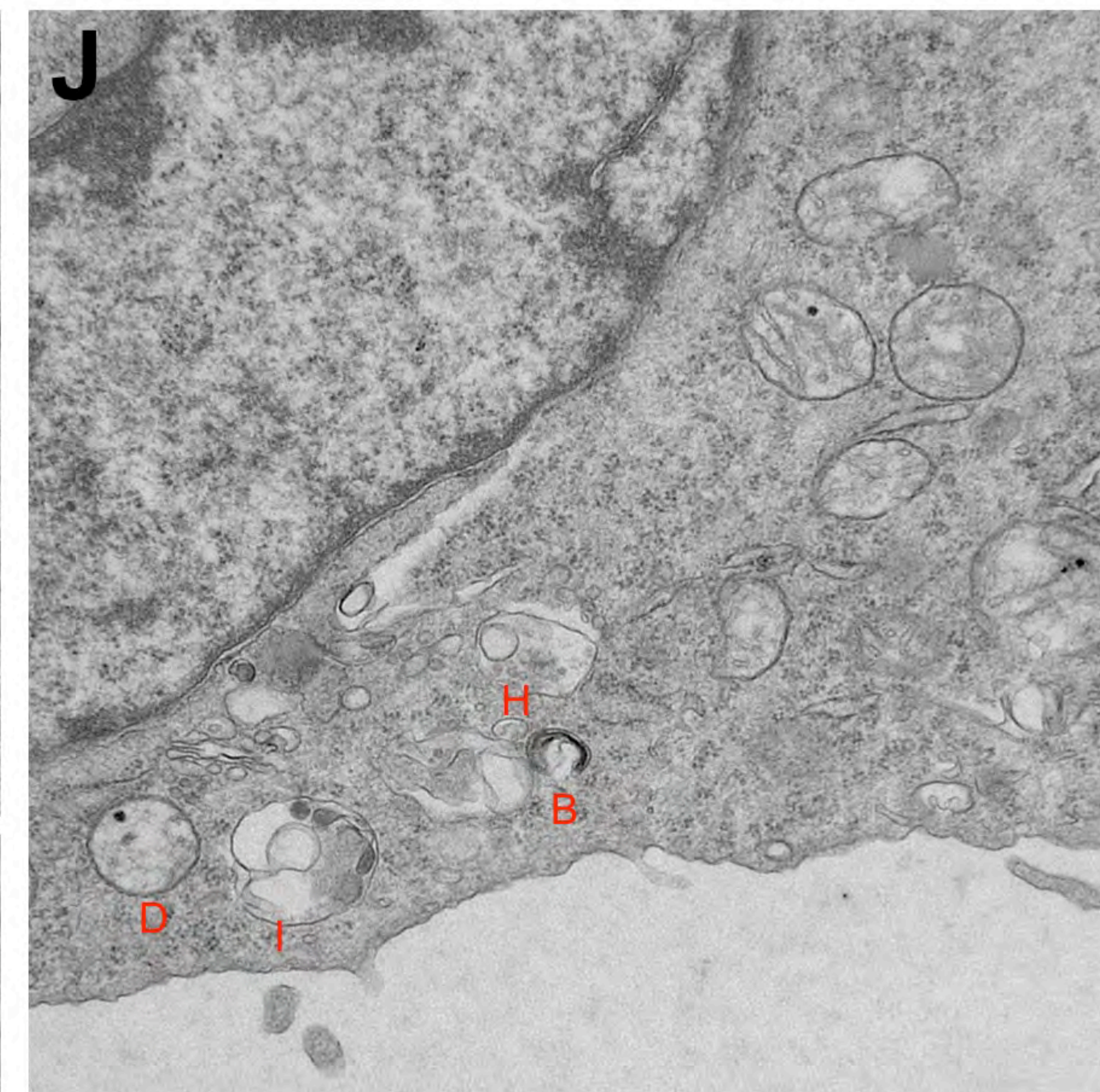
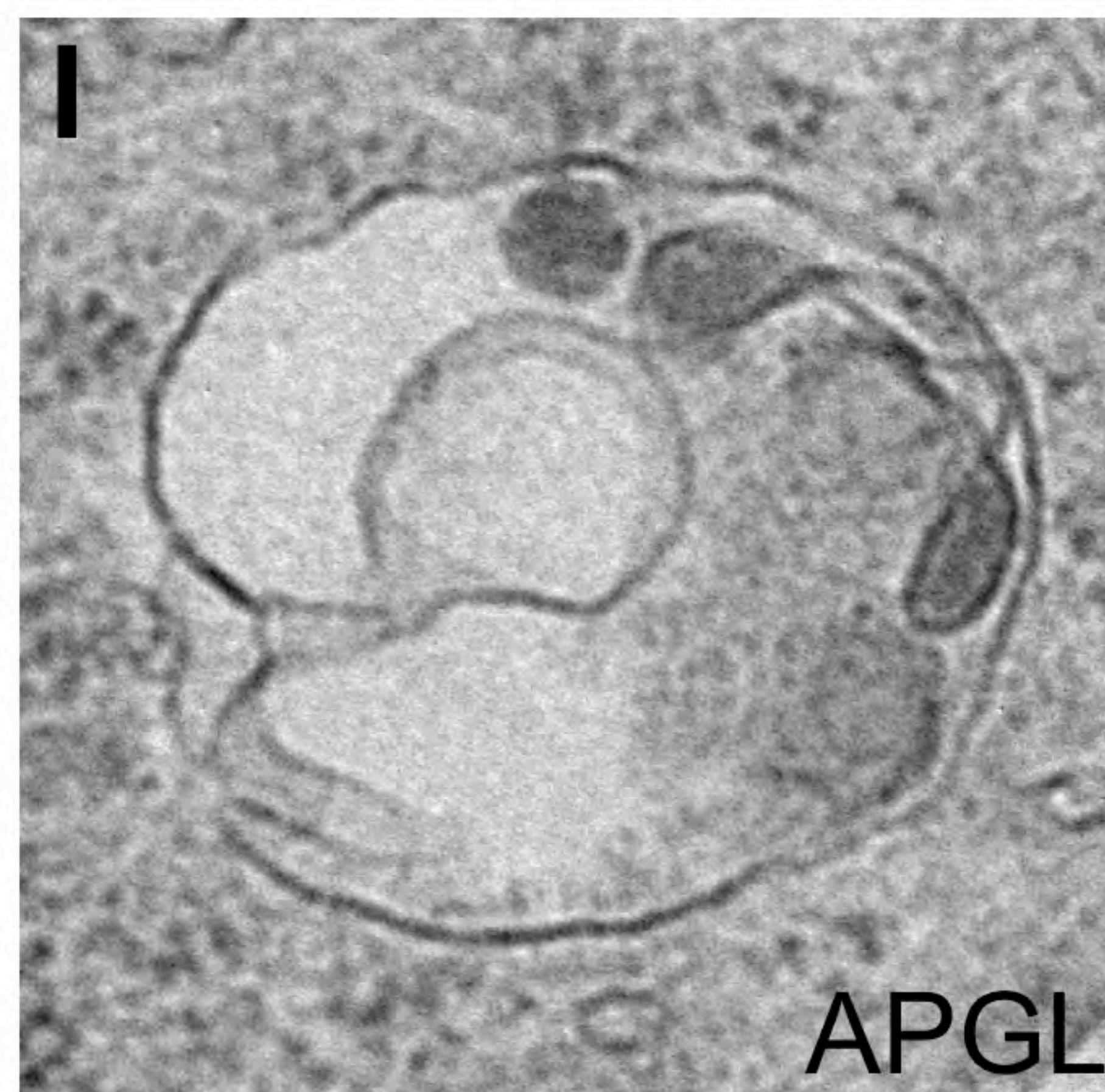
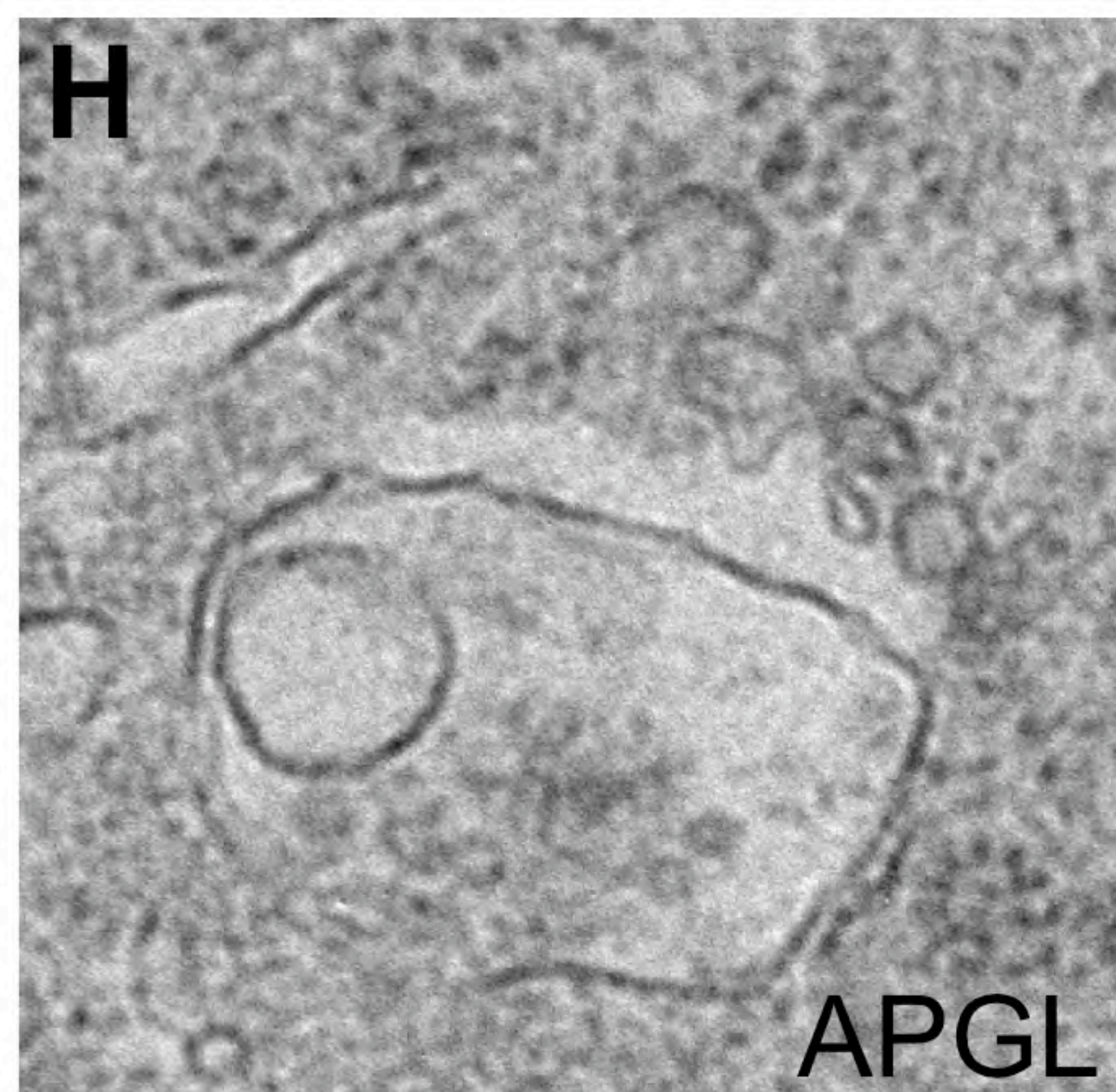
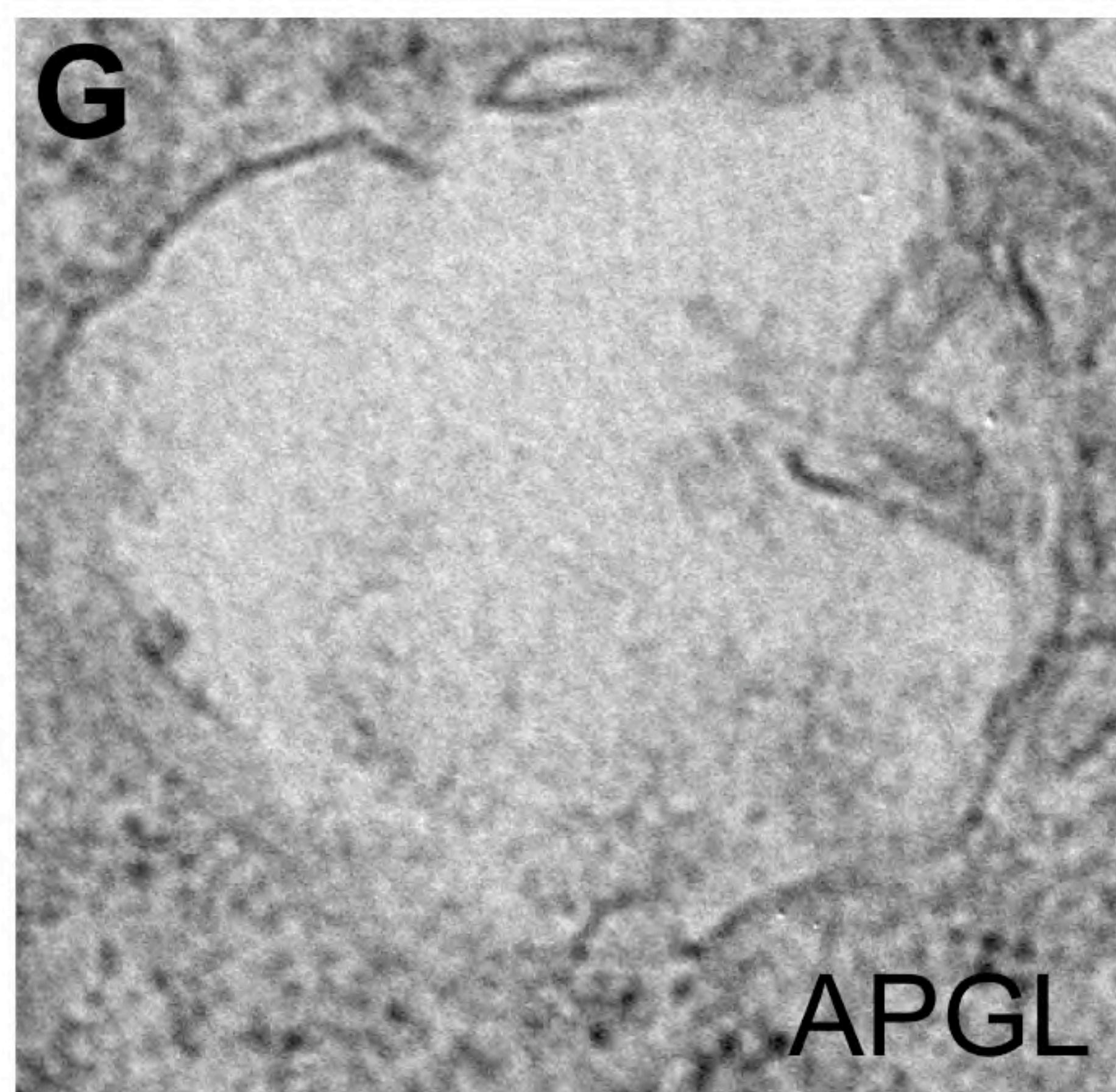
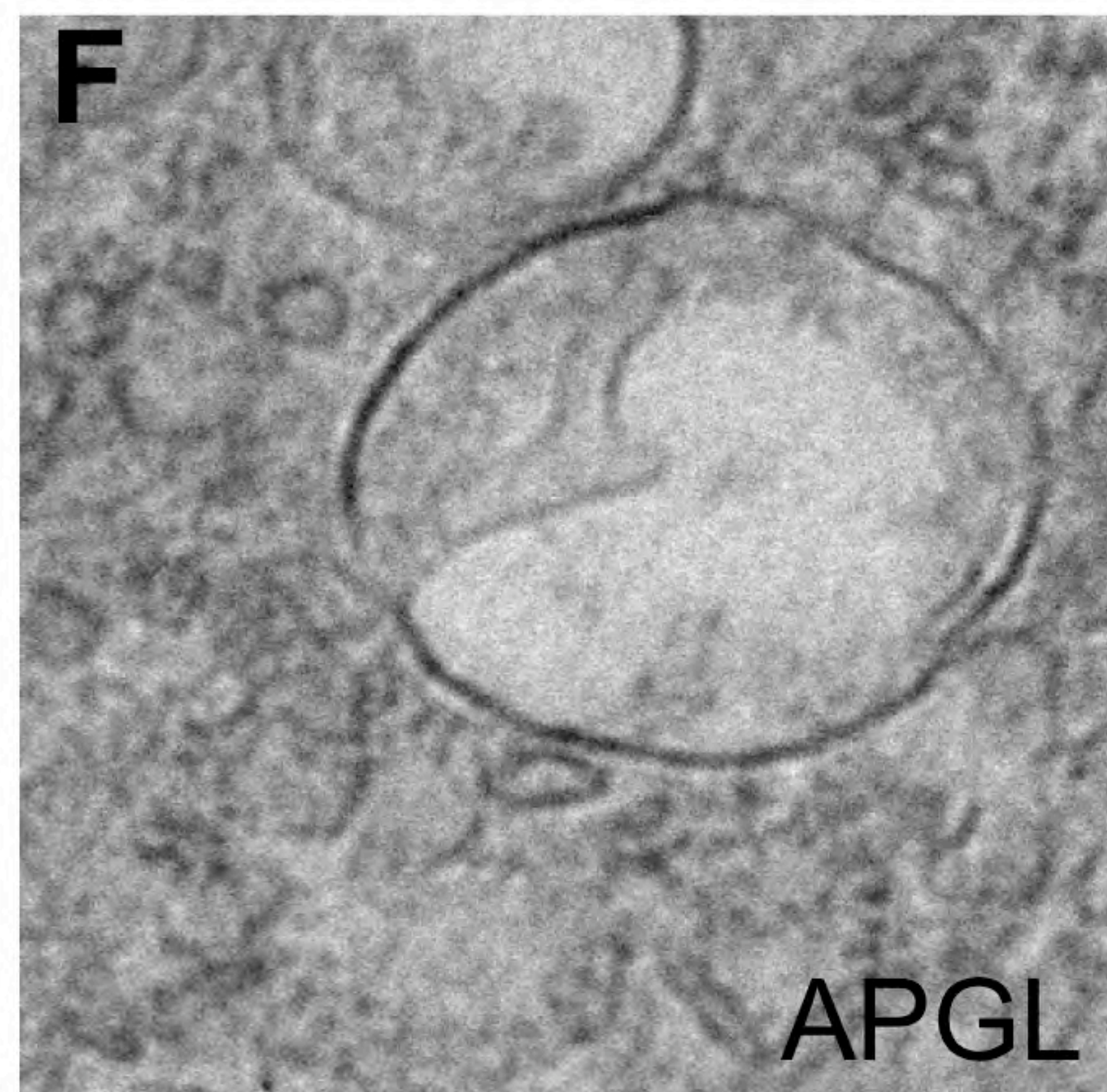
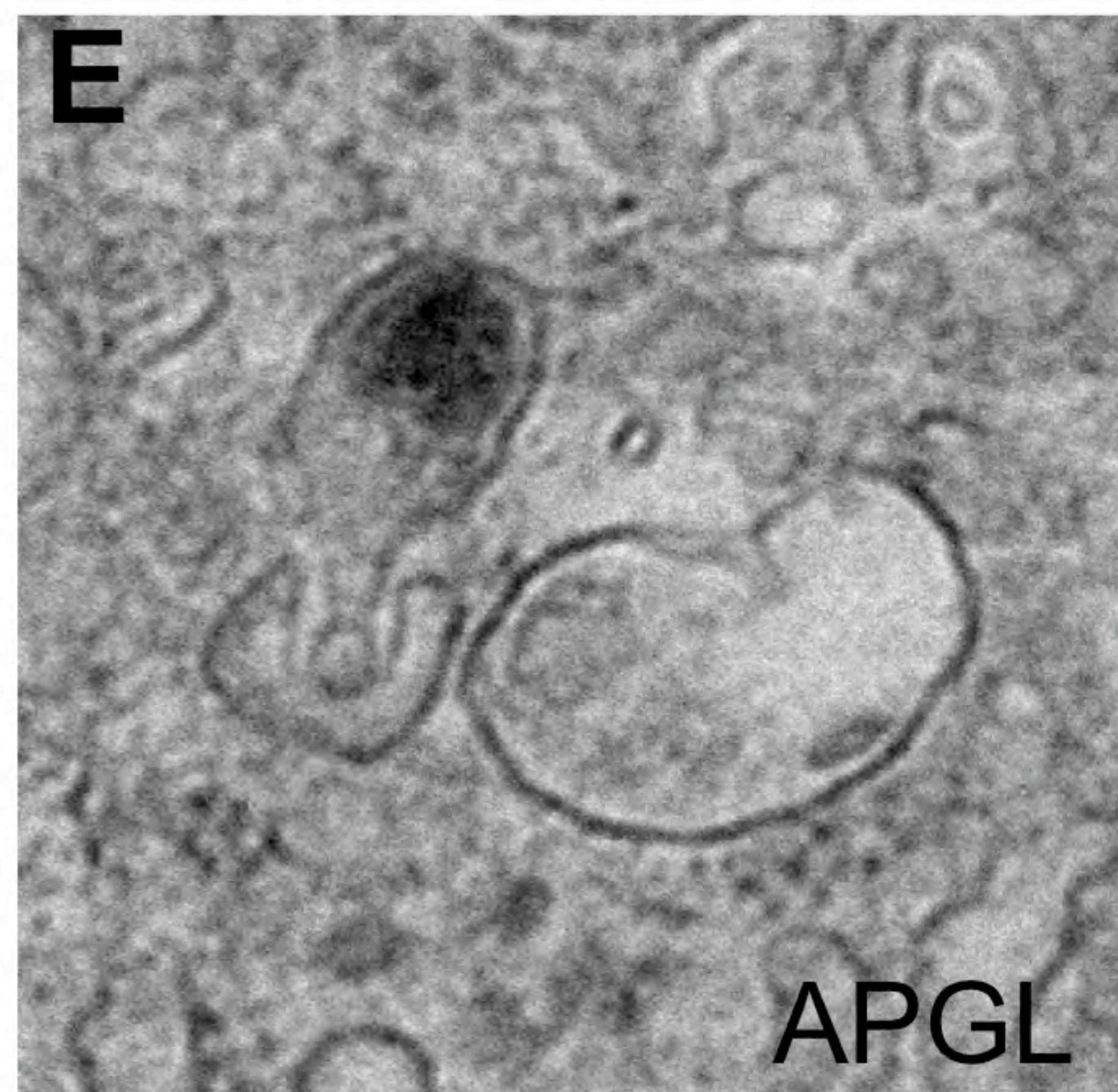
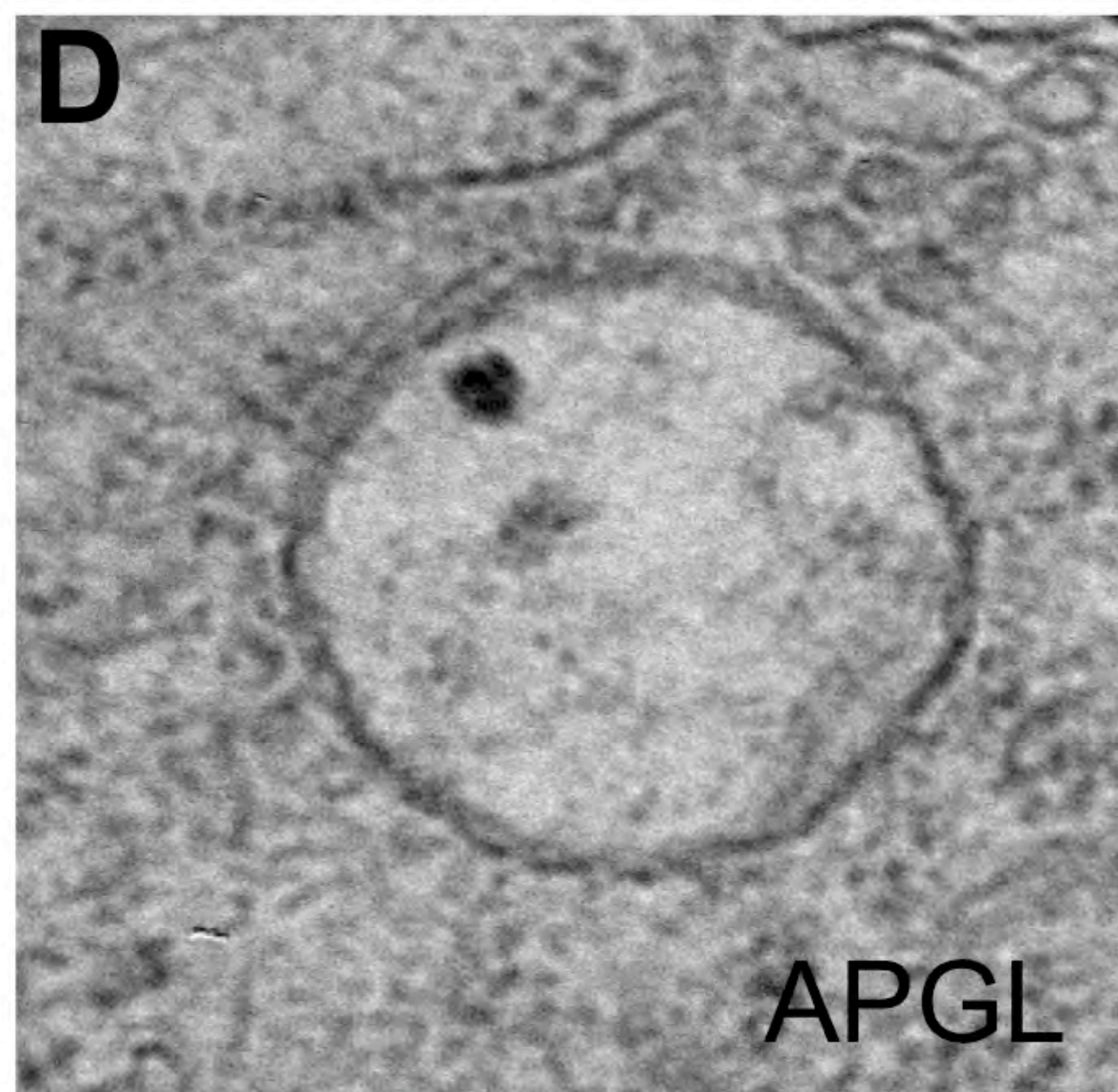
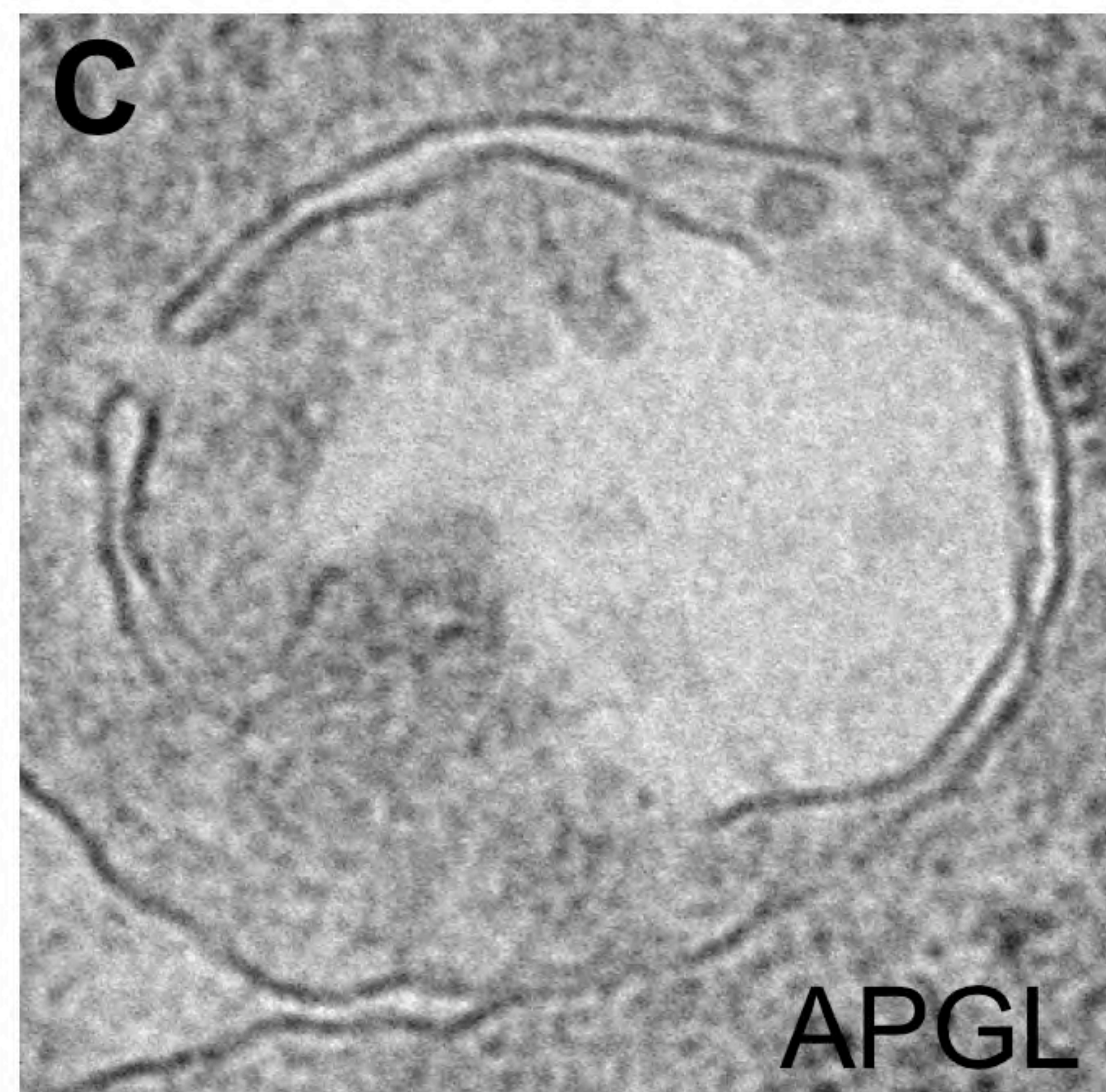
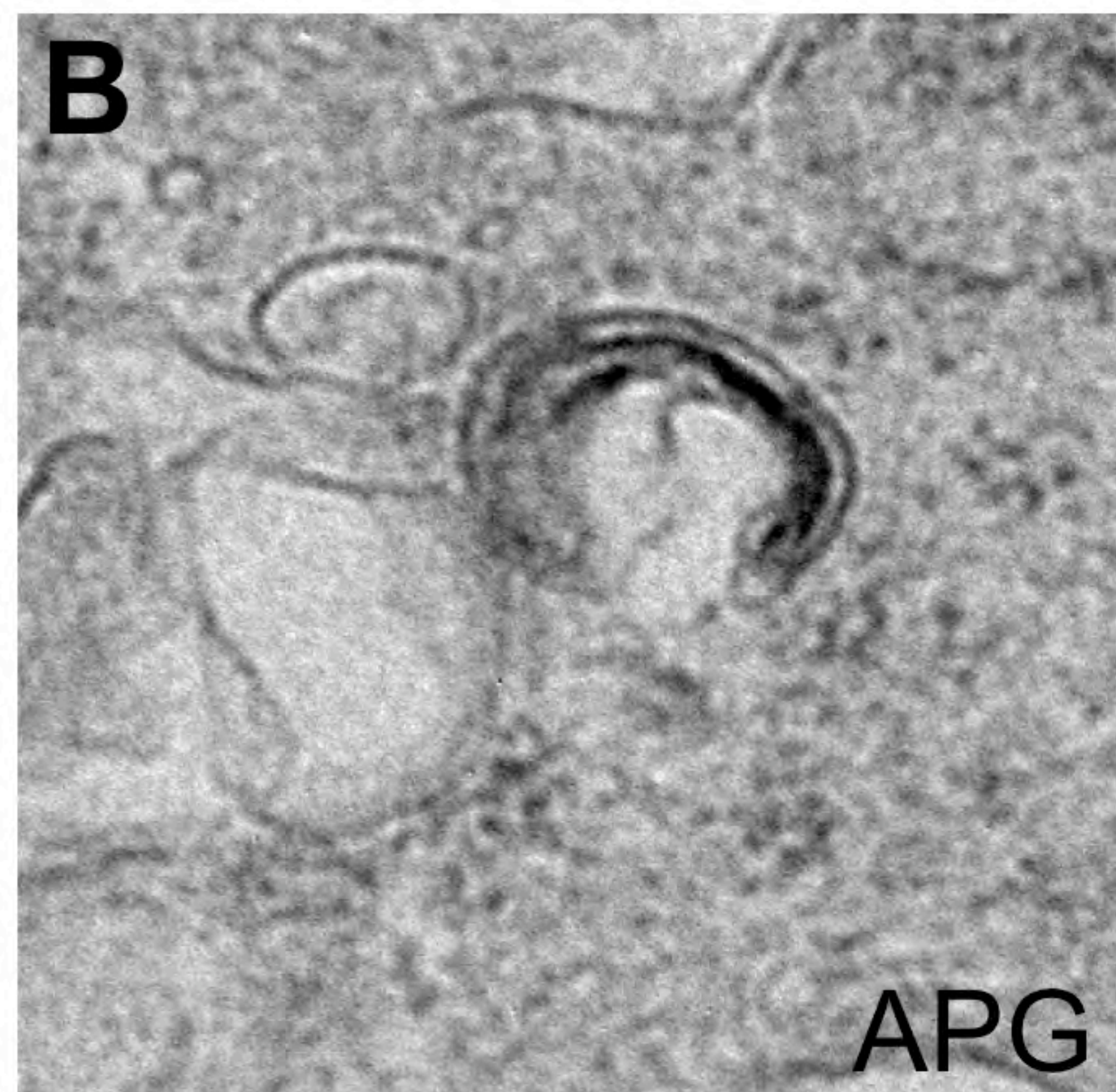
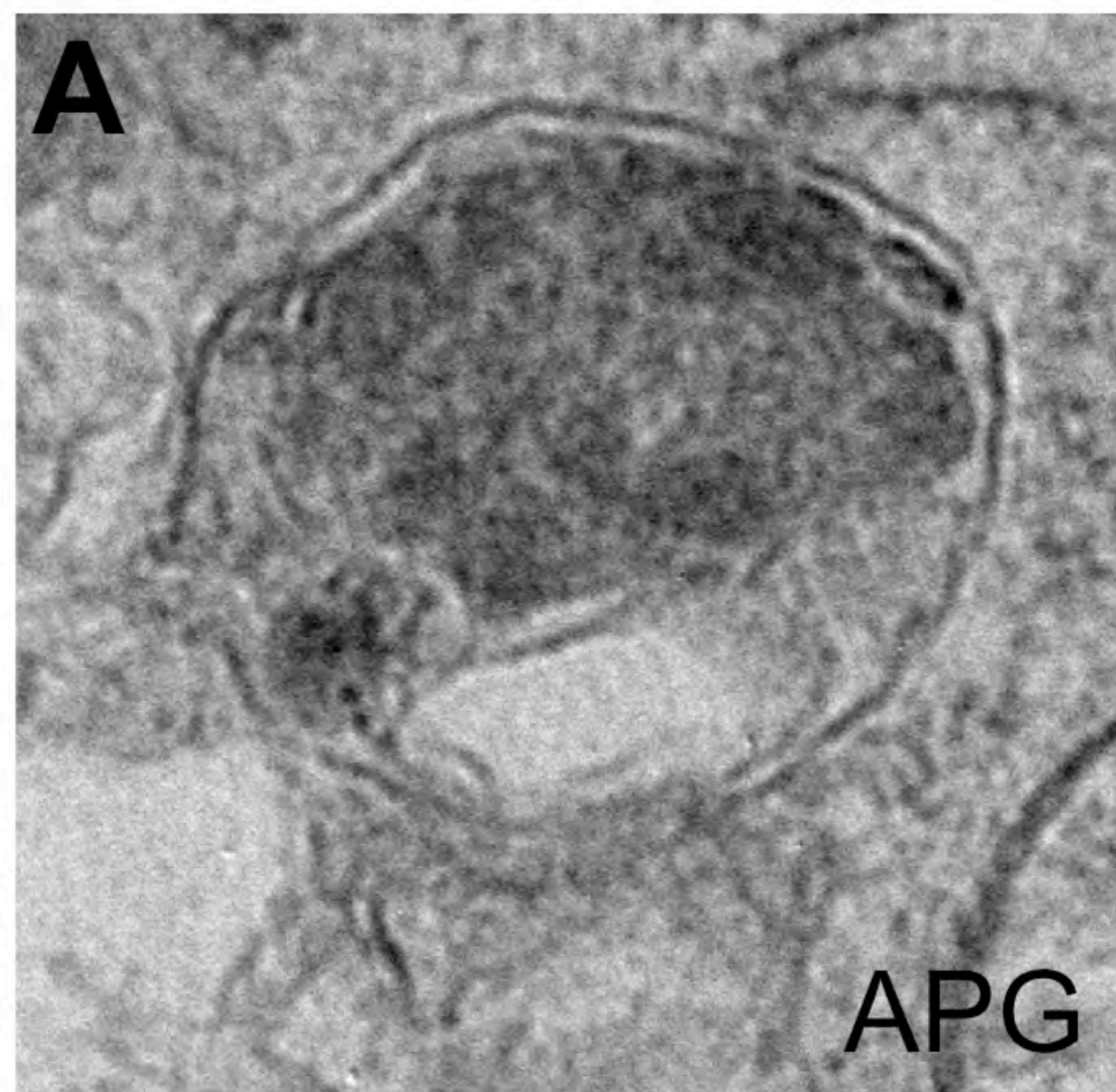
REFERENCES

- Iwata A, Riley BE, Johnston JA, Kopito RR. 2005. HDAC6 and microtubules are required for autophagic degradation of aggregated huntingtin. *J Biol Chem* **280**: 40282-40292.
- Kawaguchi Y, Kovacs JJ, McLaurin A, Vance JM, Ito A, Yao TP. 2003. The deacetylase HDAC6 regulates aggresome formation and cell viability in response to misfolded protein stress. *Cell* **115**: 727-738.
- Marzella L, Ahlberg J, Glaumann H. 1982. Isolation of autophagic vacuoles from rat liver: morphological and biochemical characterization. *J Cell Biol* **93**: 144-154.
- Pattingre S, Petiot A, Codogno P. 2004. Analyses of Galpha-interacting protein and activator of G-protein-signaling-3 functions in macroautophagy. *Methods Enzymol* **390**: 17-31.
- Yu WH, Cuervo AM, Kumar A, Peterhoff CM, Schmidt SD, Lee JH, Mohan PS, Mercken M, Farmery MR, Tjernberg LO et al. 2005. Macroautophagy--a novel Beta-amyloid peptide-generating pathway activated in Alzheimer's disease. *J Cell Biol* **171**: 87-98.

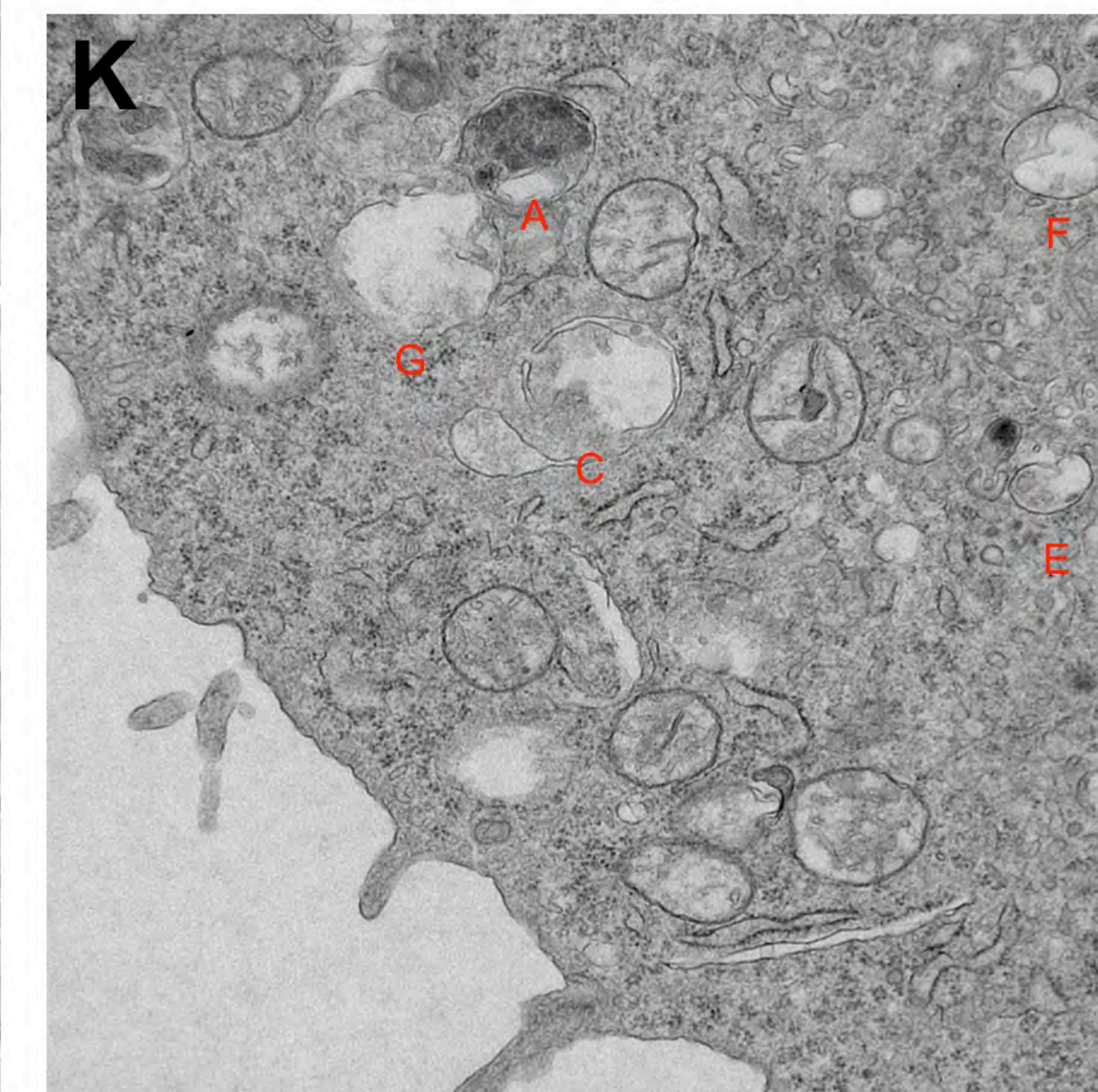
A**B**

A**B****C**



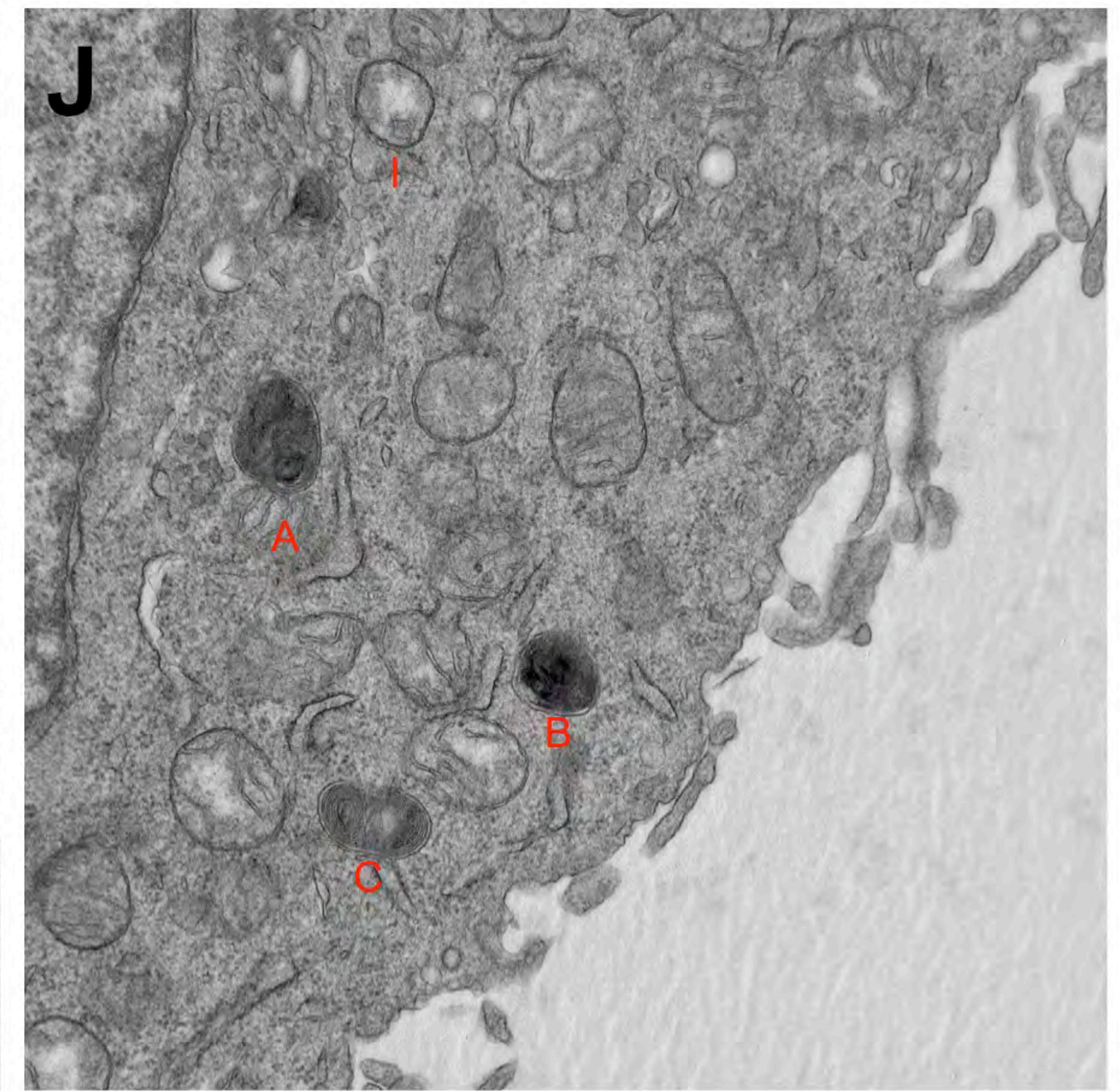
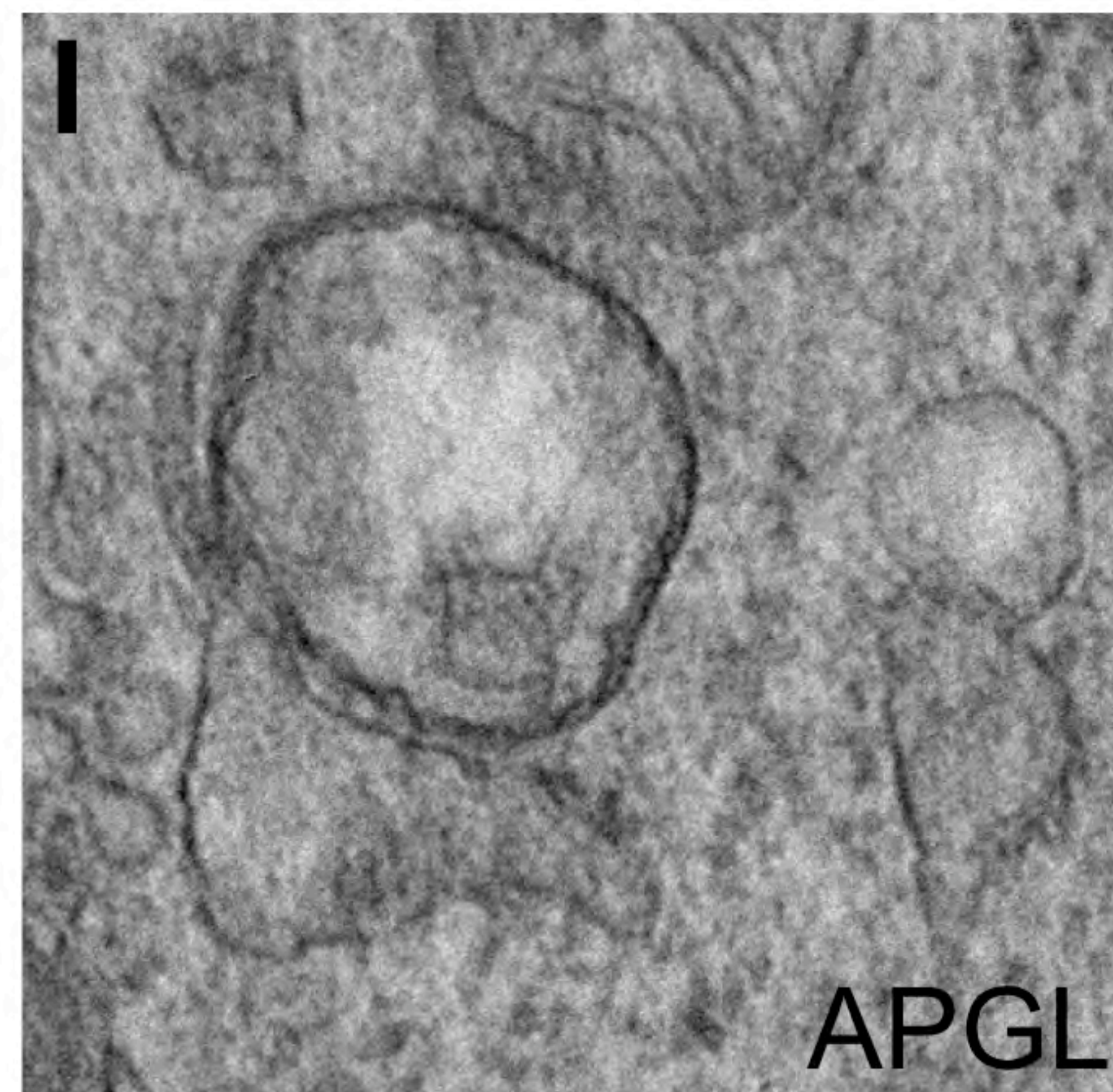
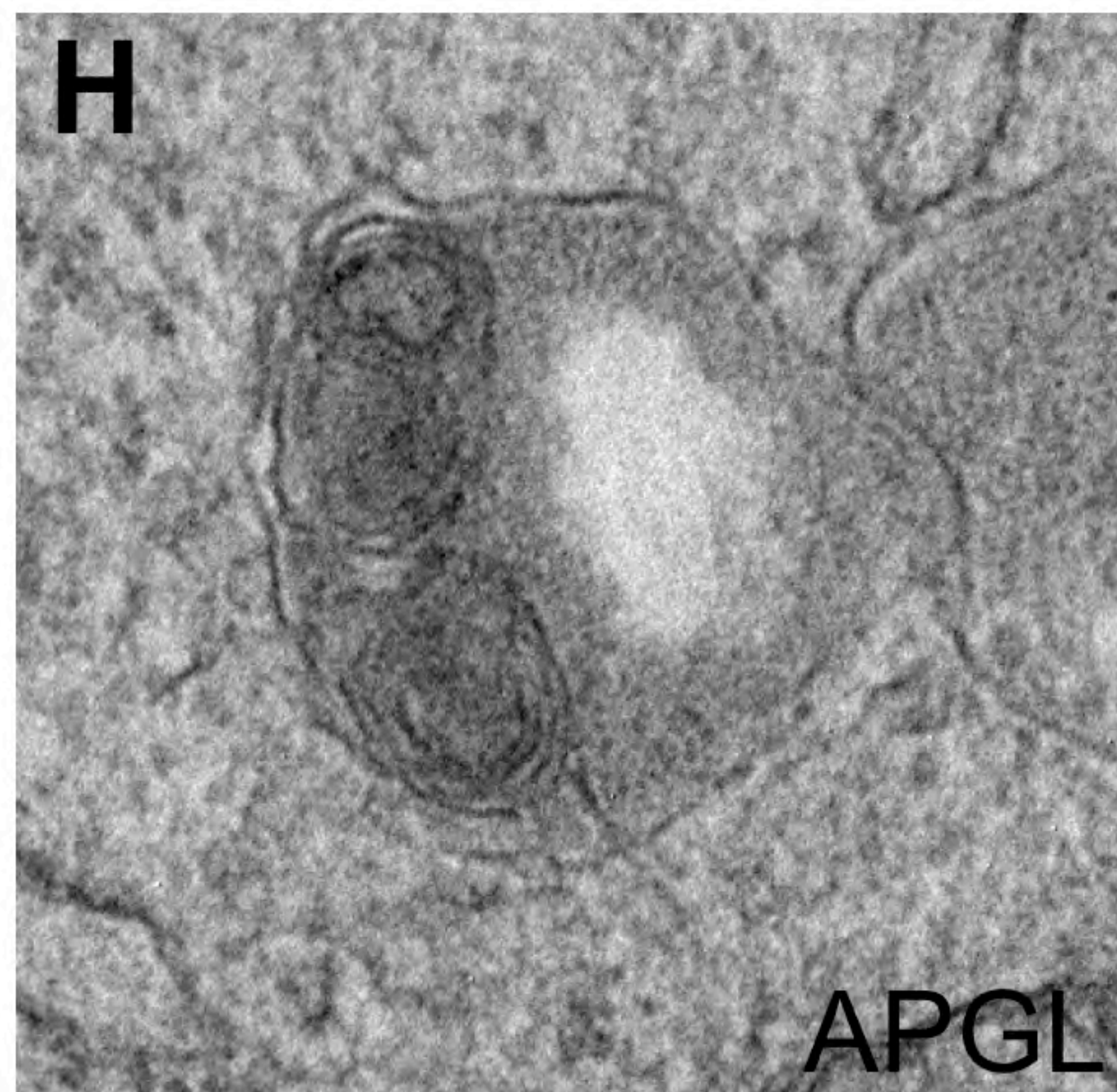
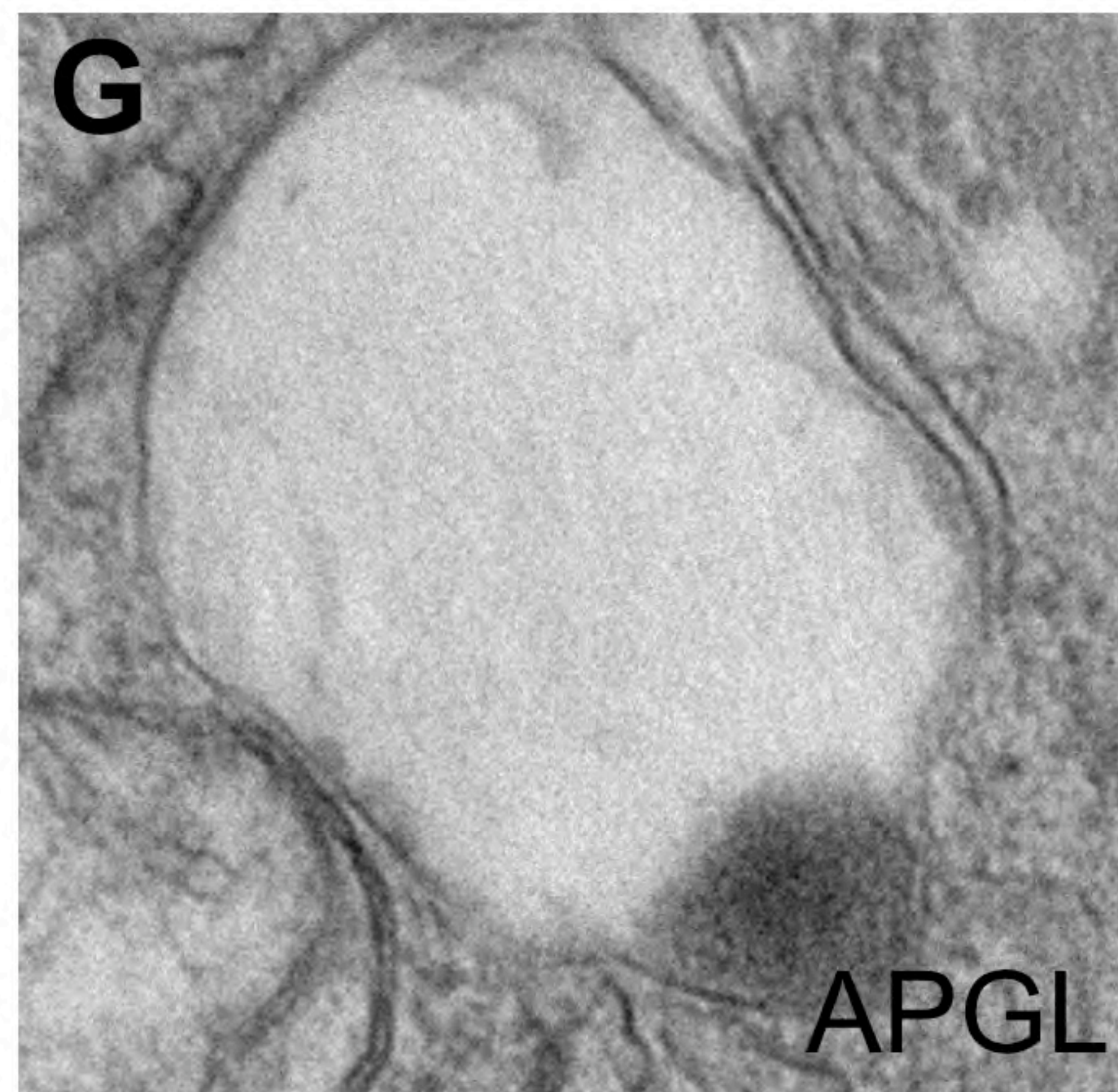
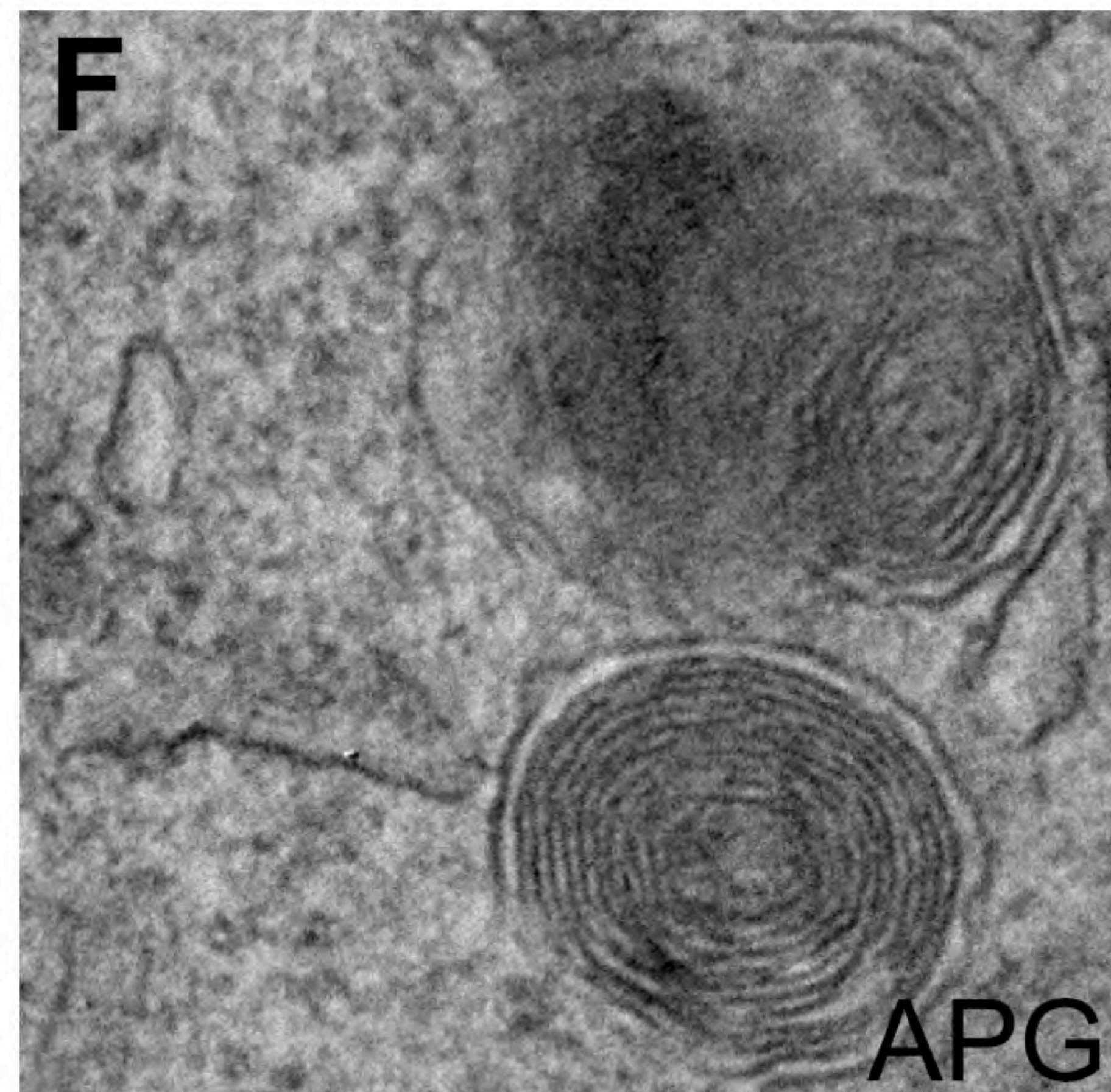
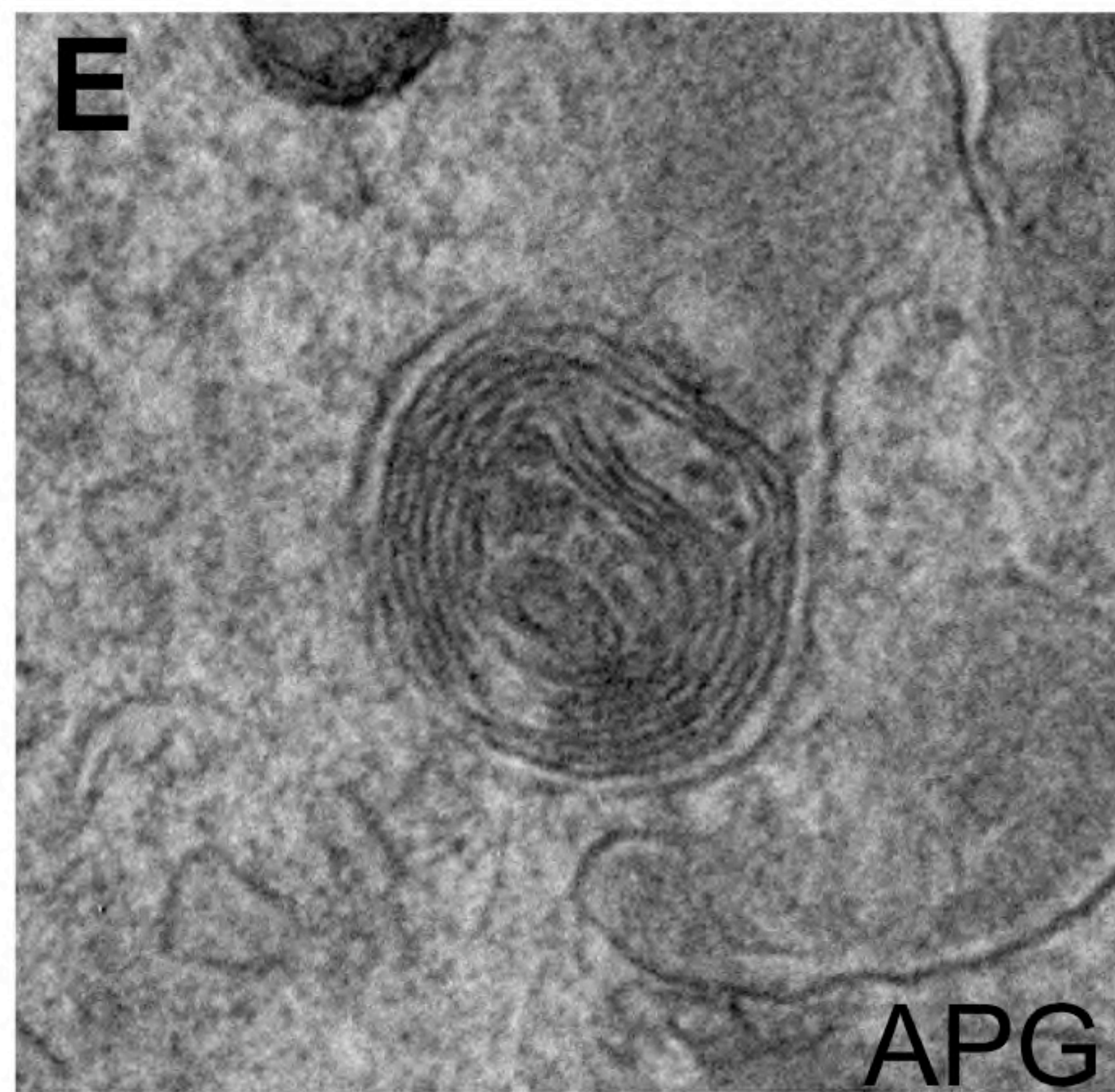
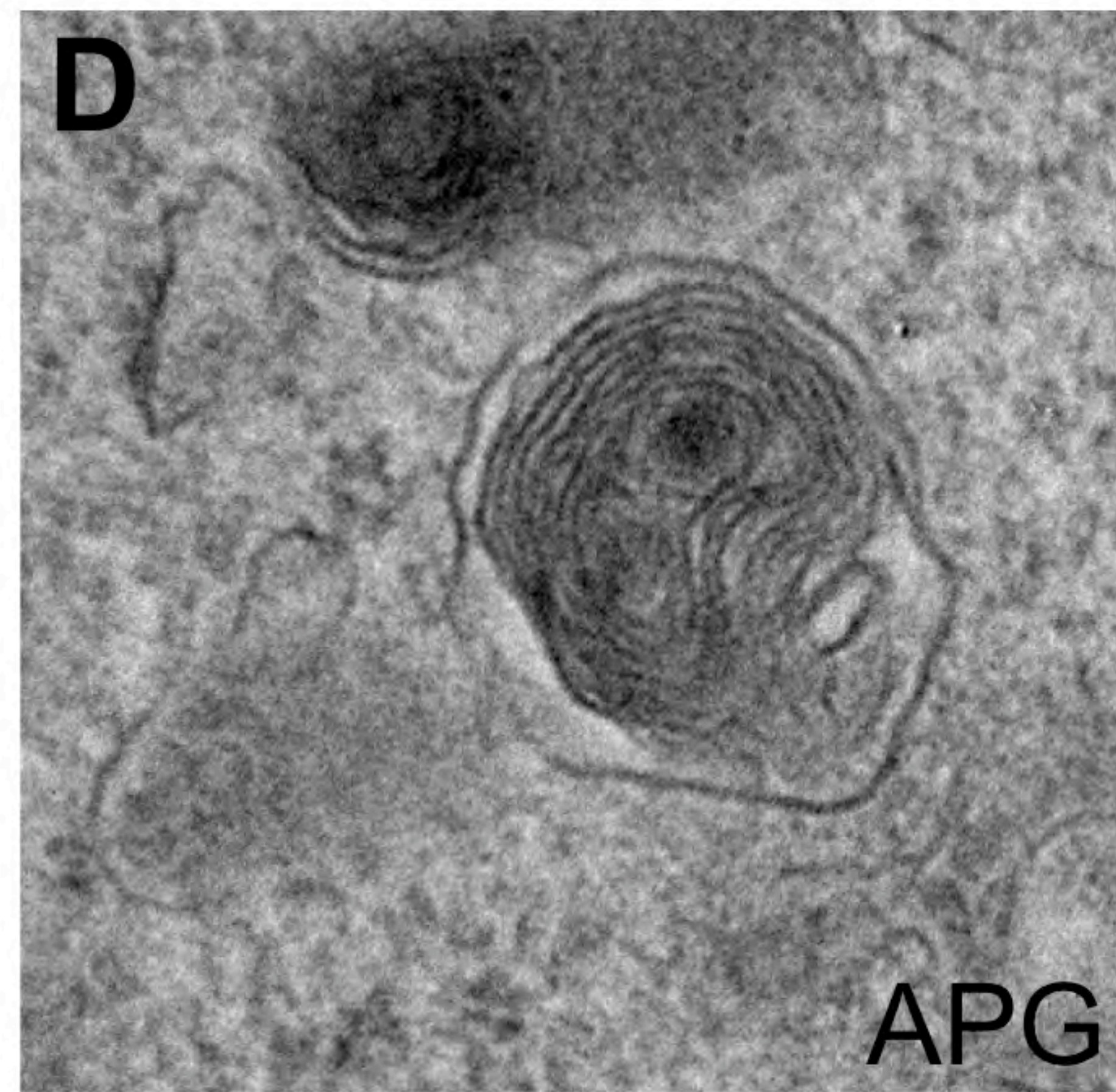
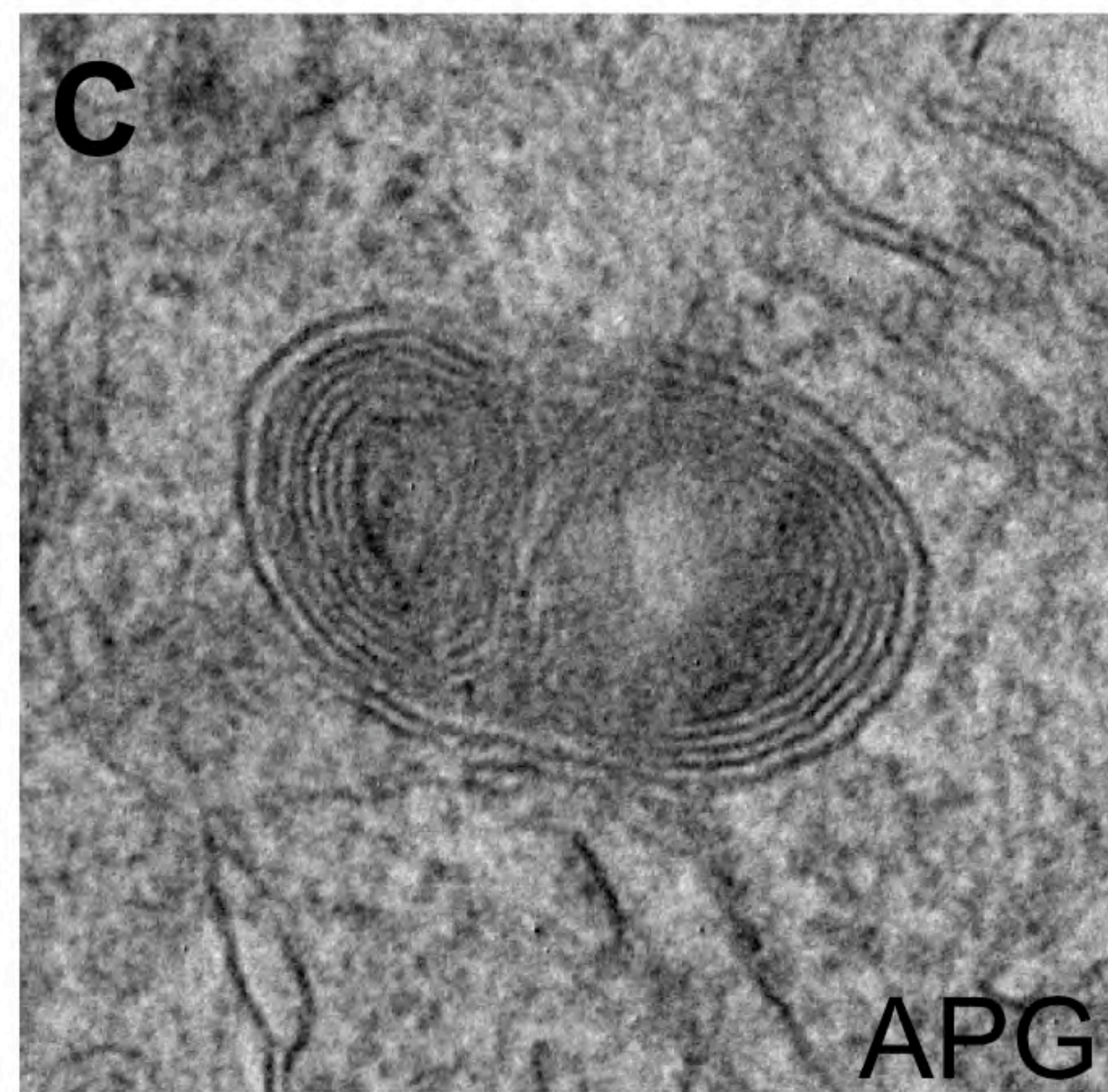
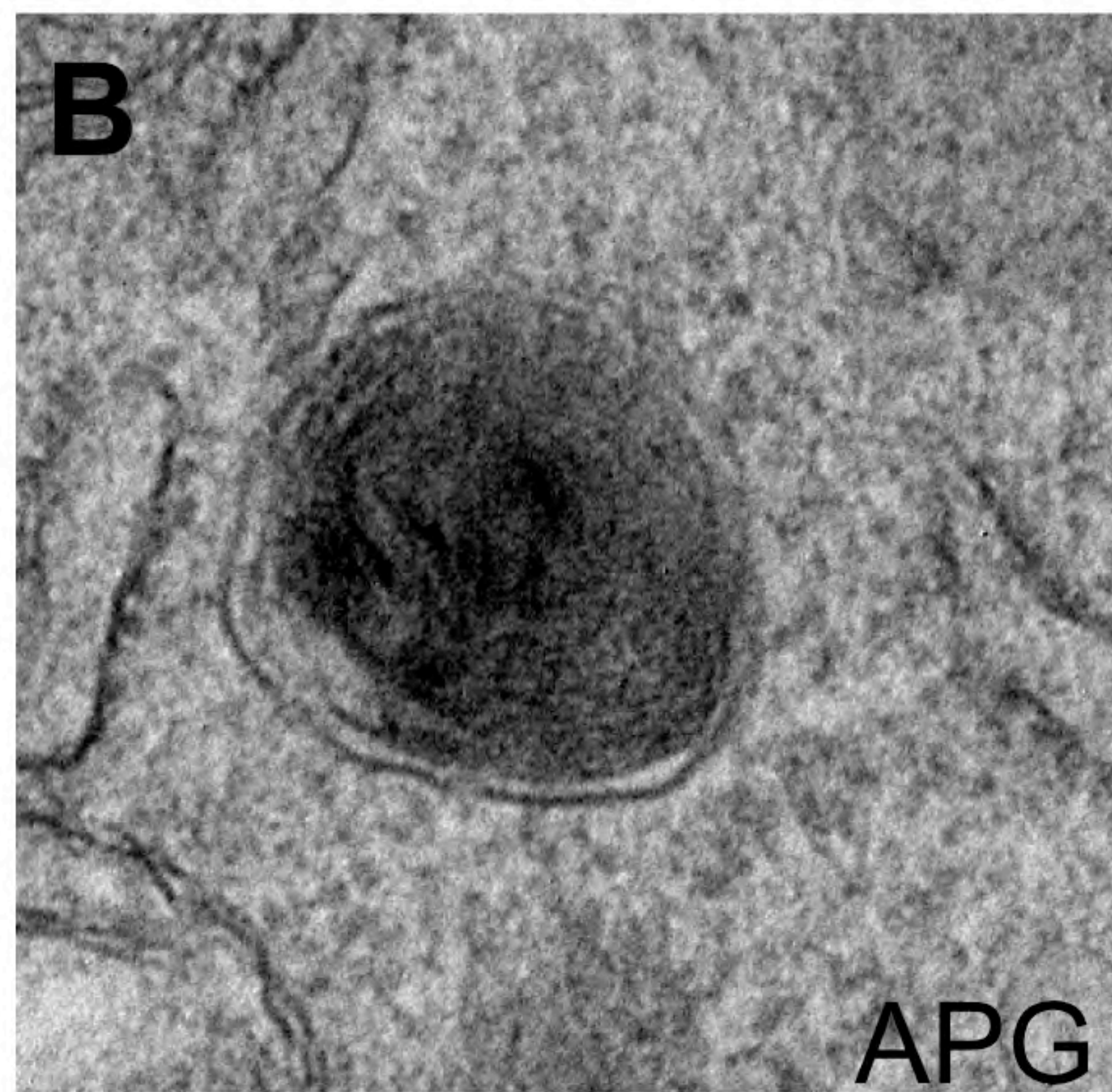
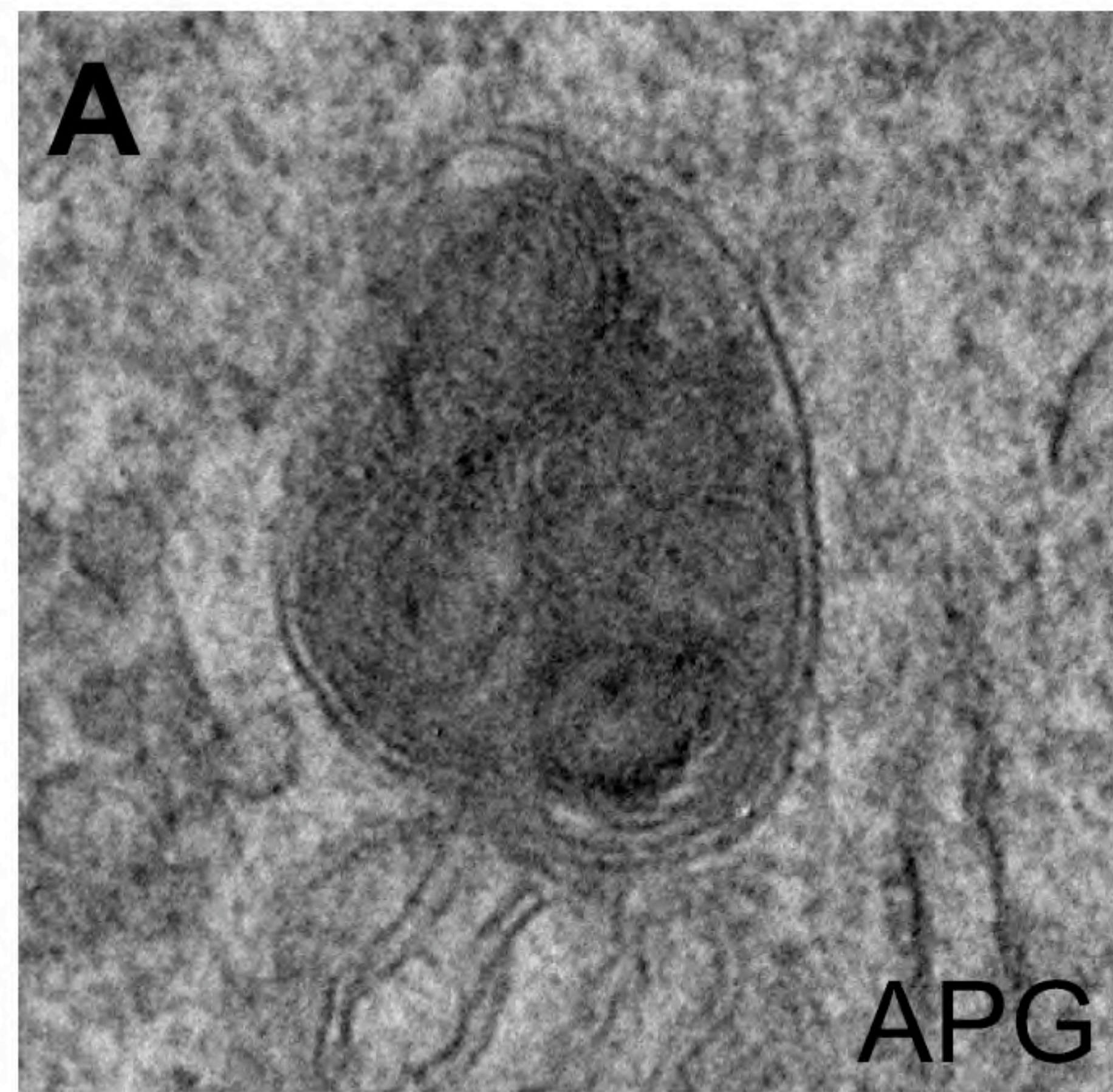


500 nm
HV=80kV
Direct Mag: 10000x

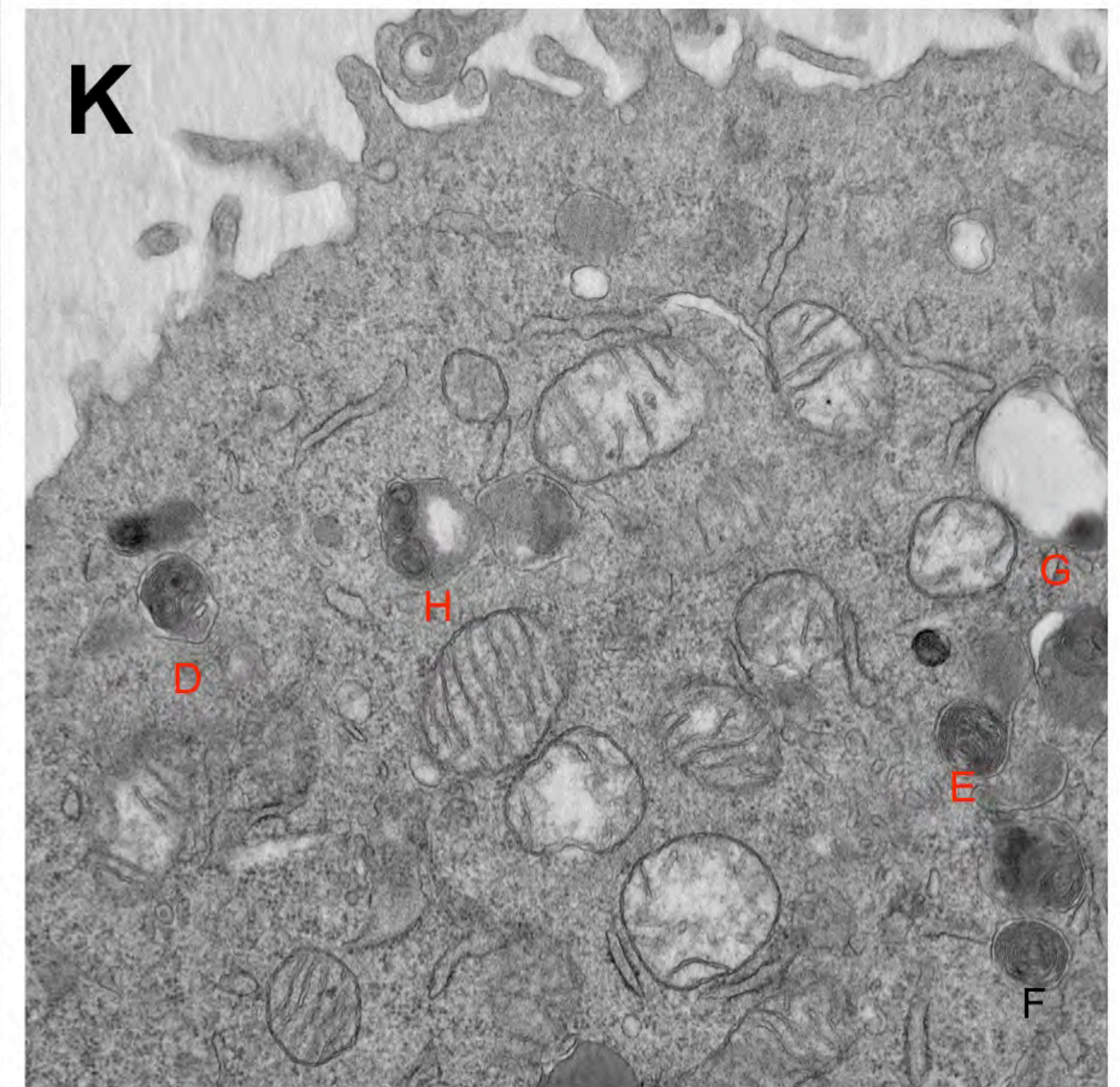


500 nm
HV=80kV
Direct Mag: 10000x

500 nm

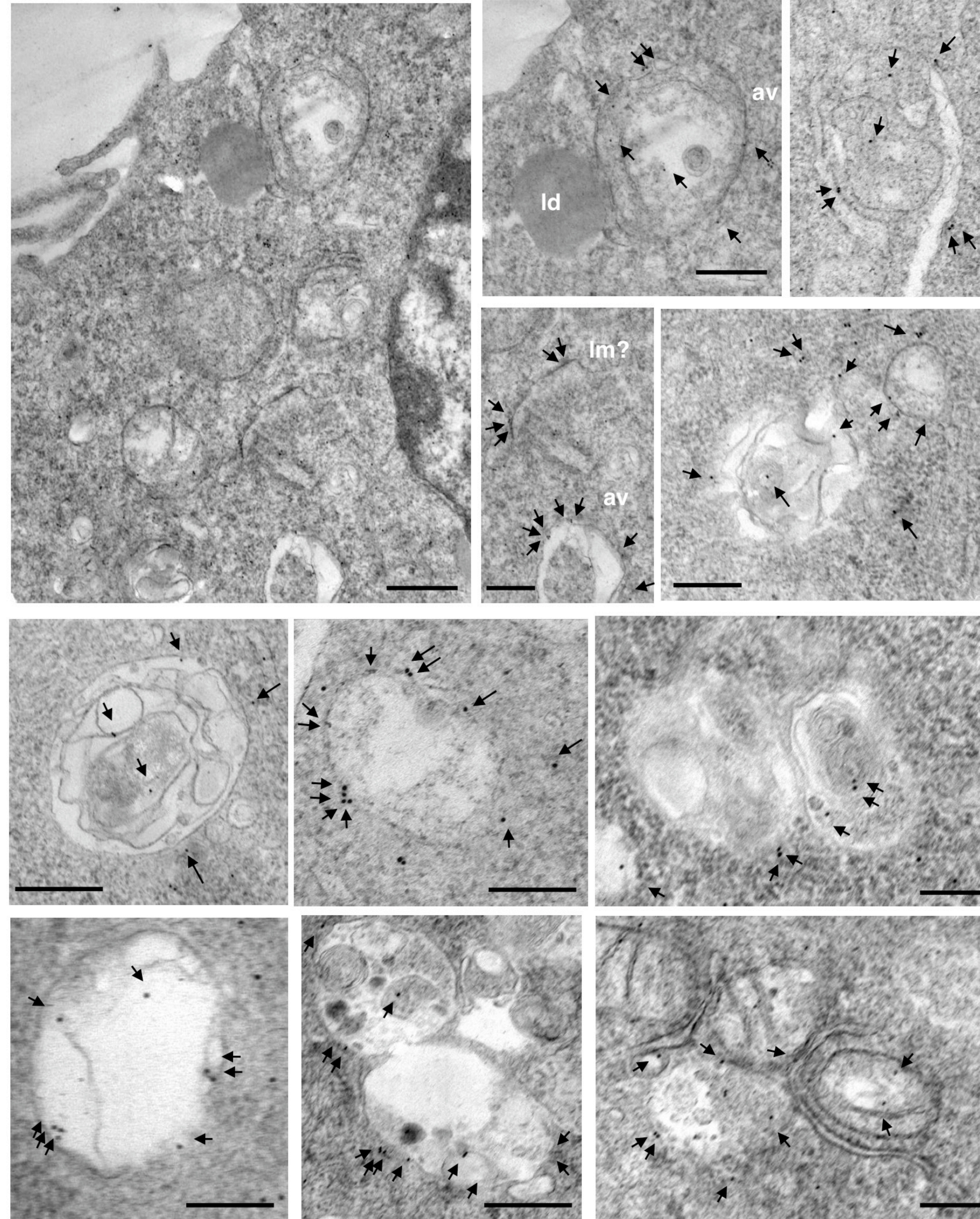


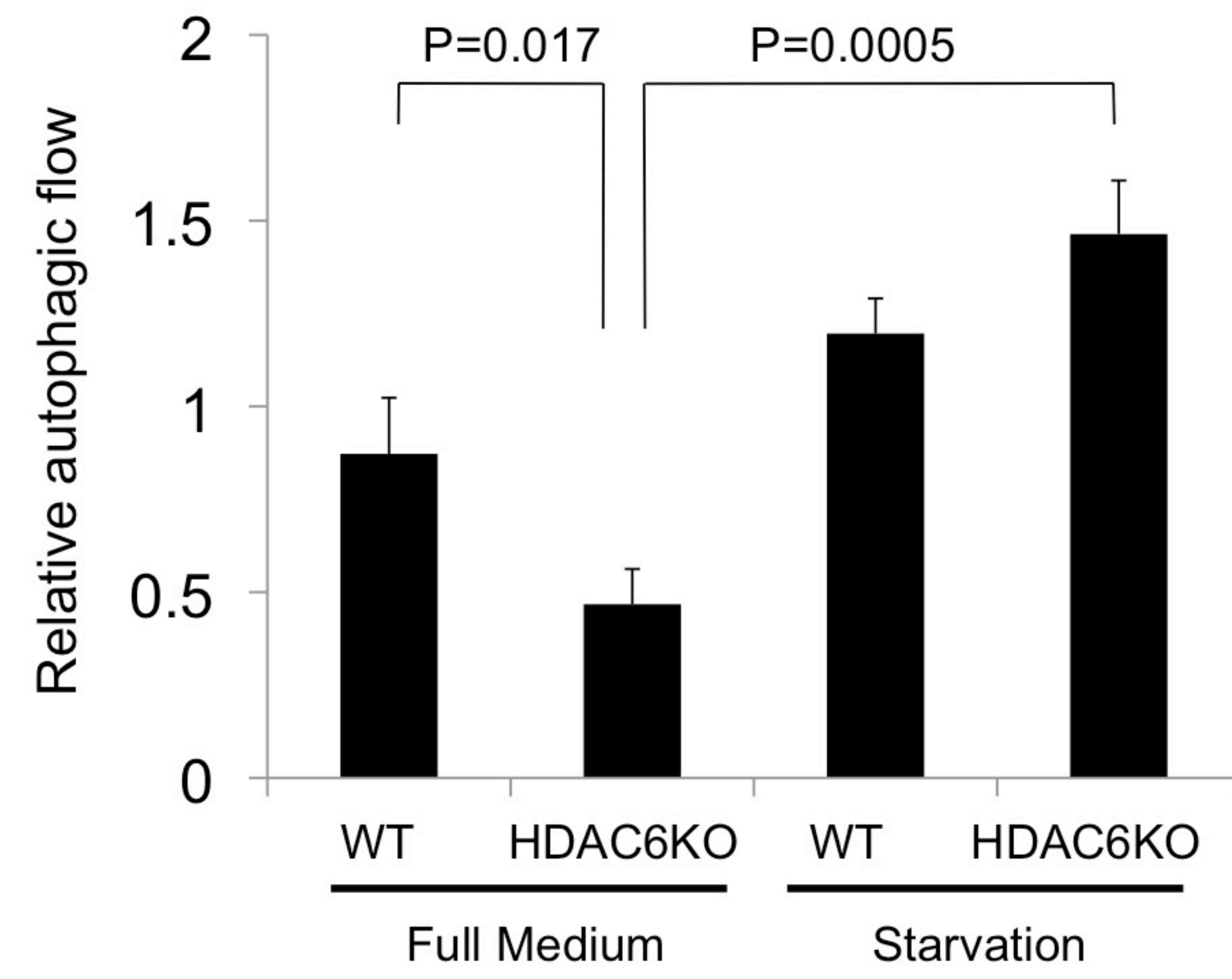
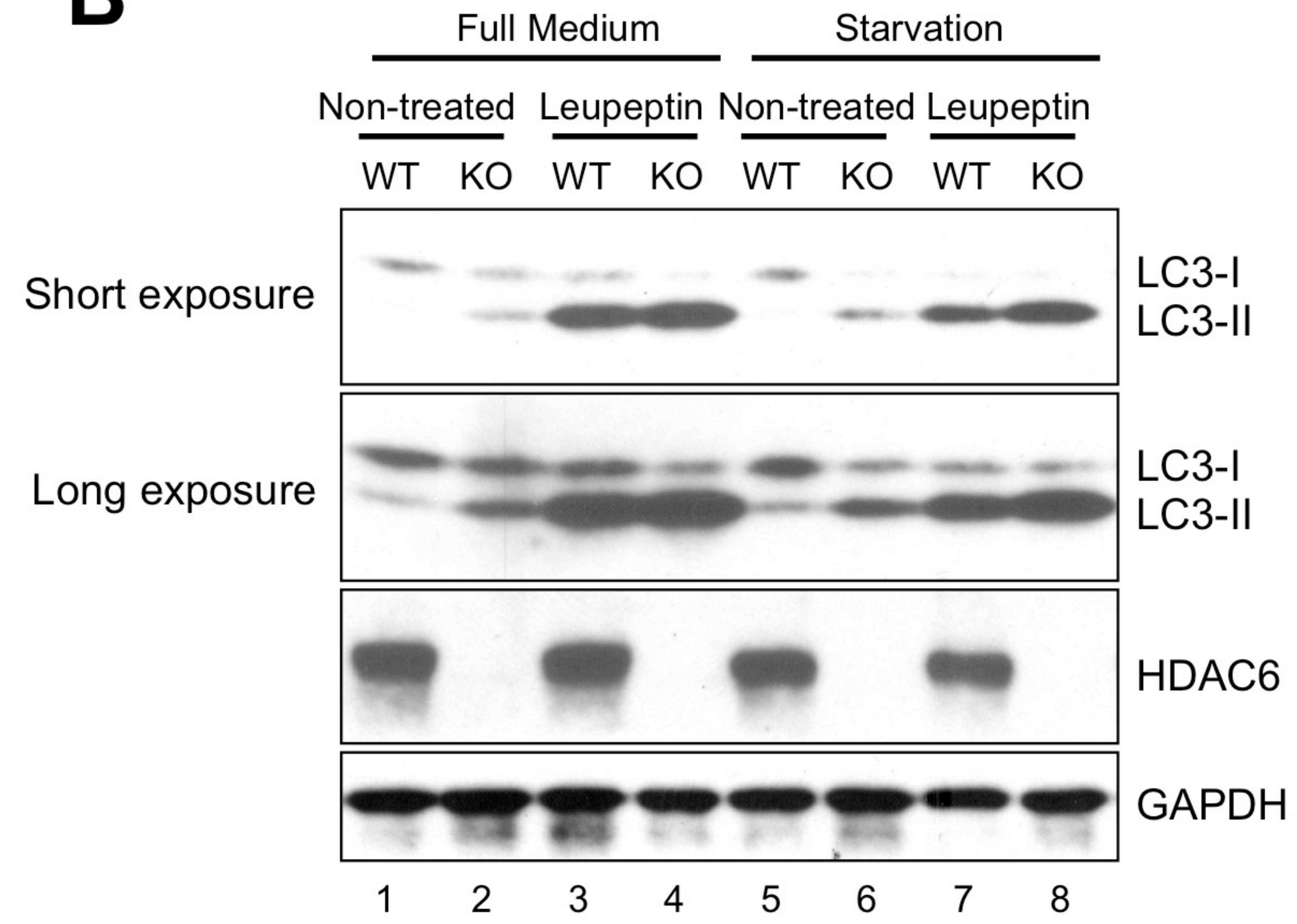
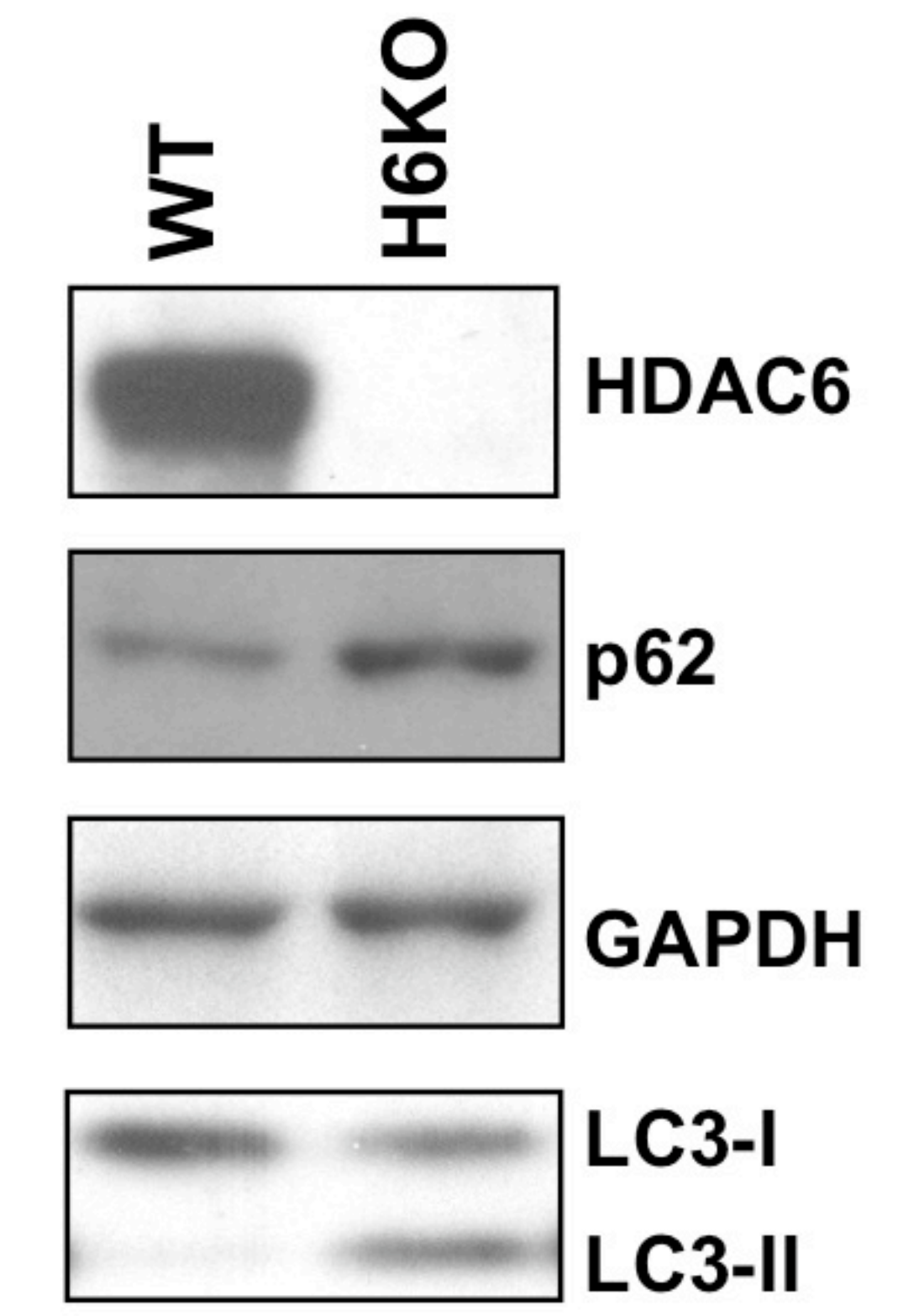
500 nm
HV=80kV
Direct Mag: 10000x

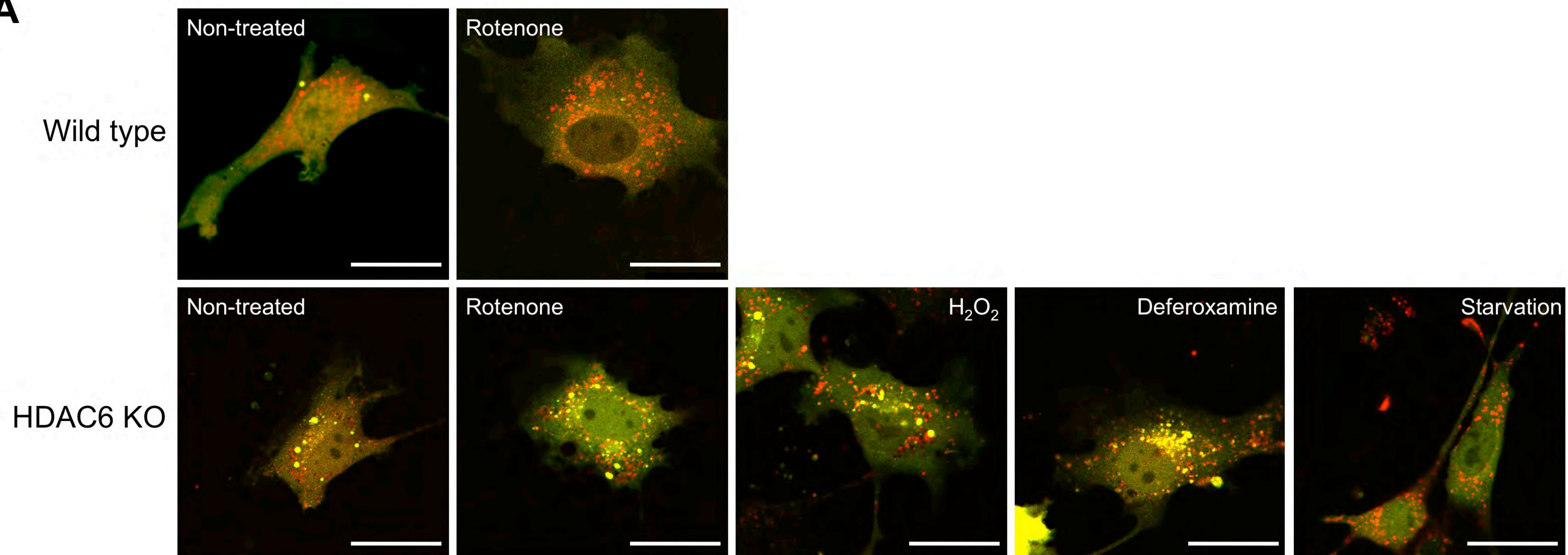
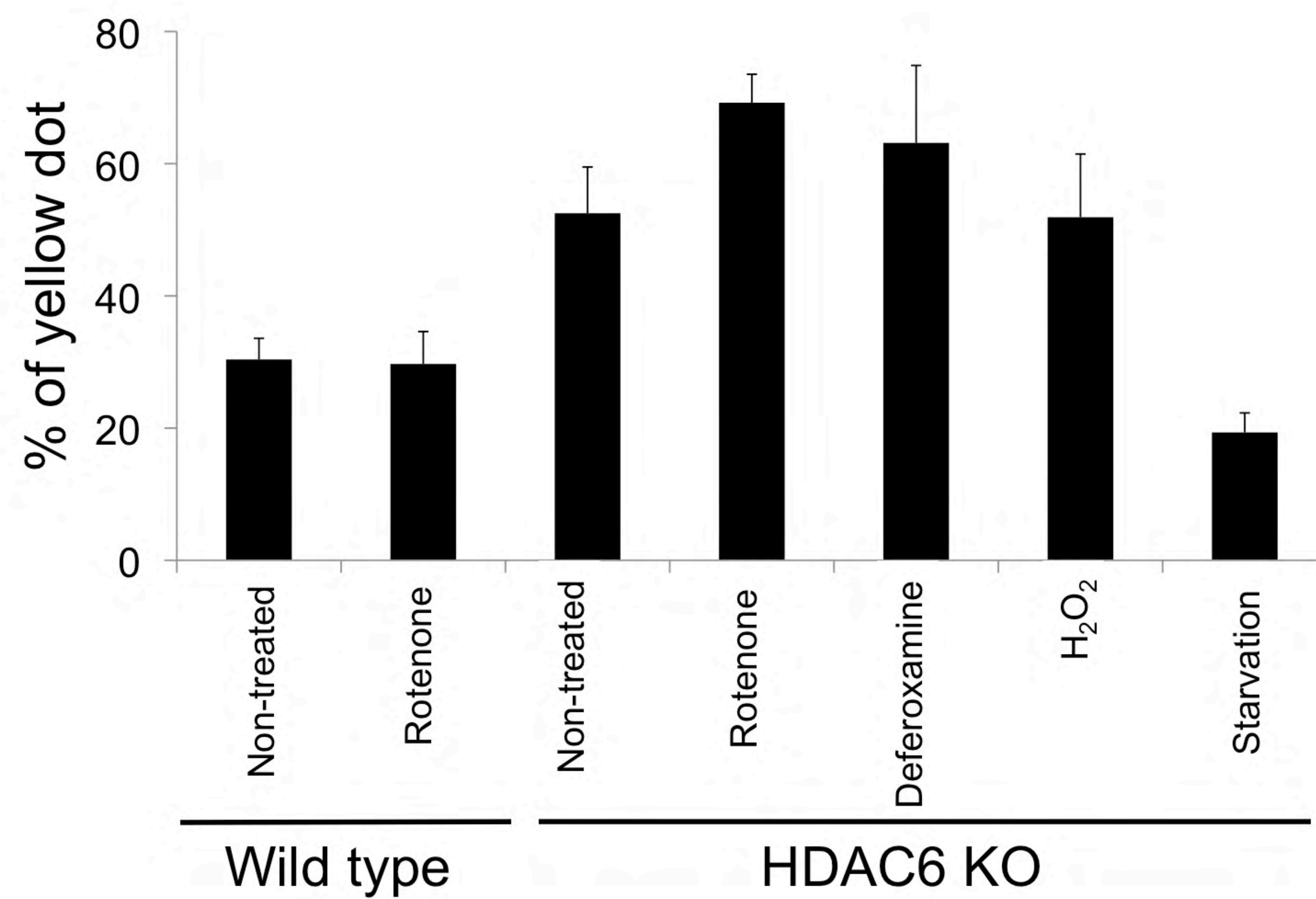


500 nm
HV=80kV
Direct Mag: 10000x

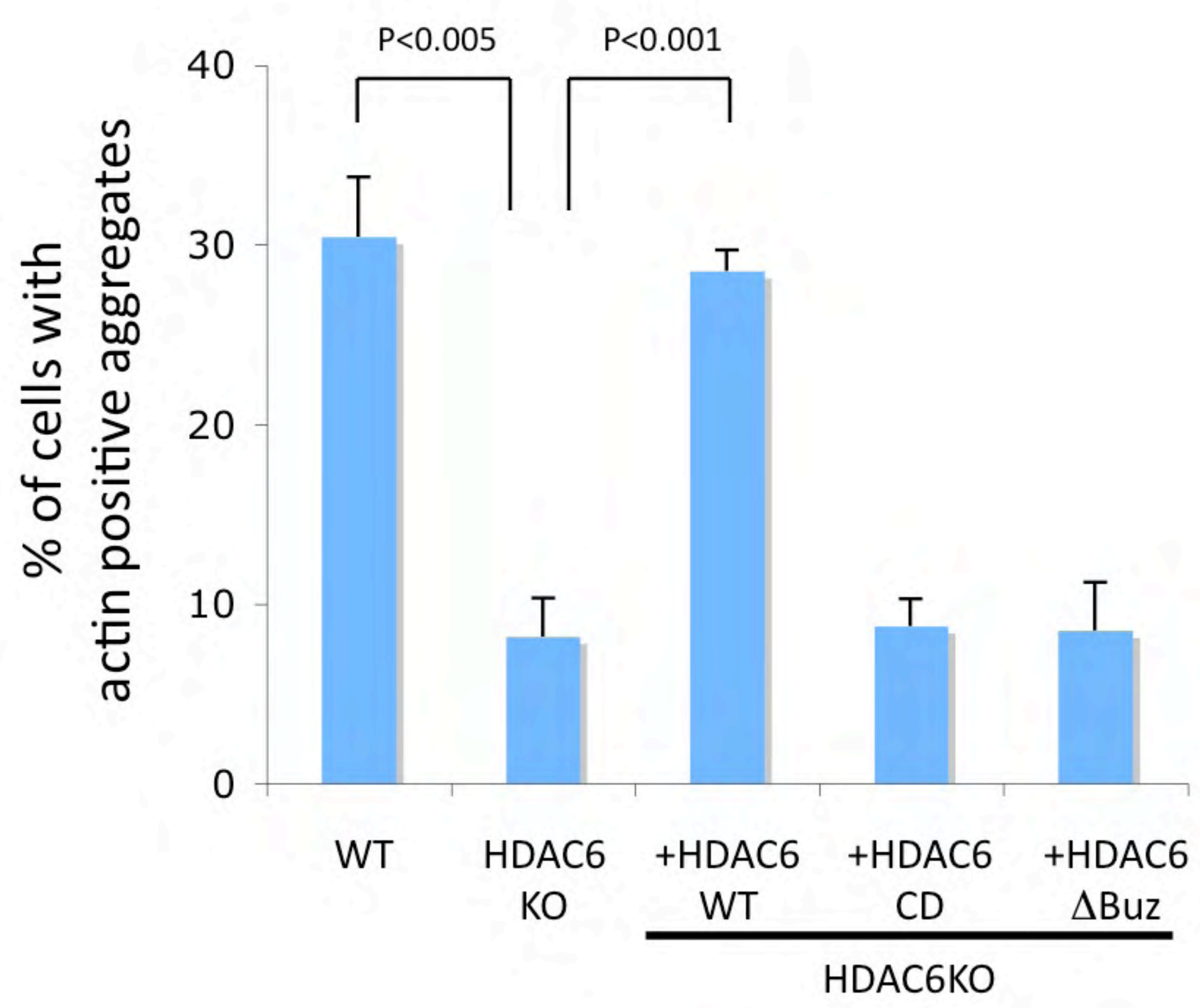
500 nm



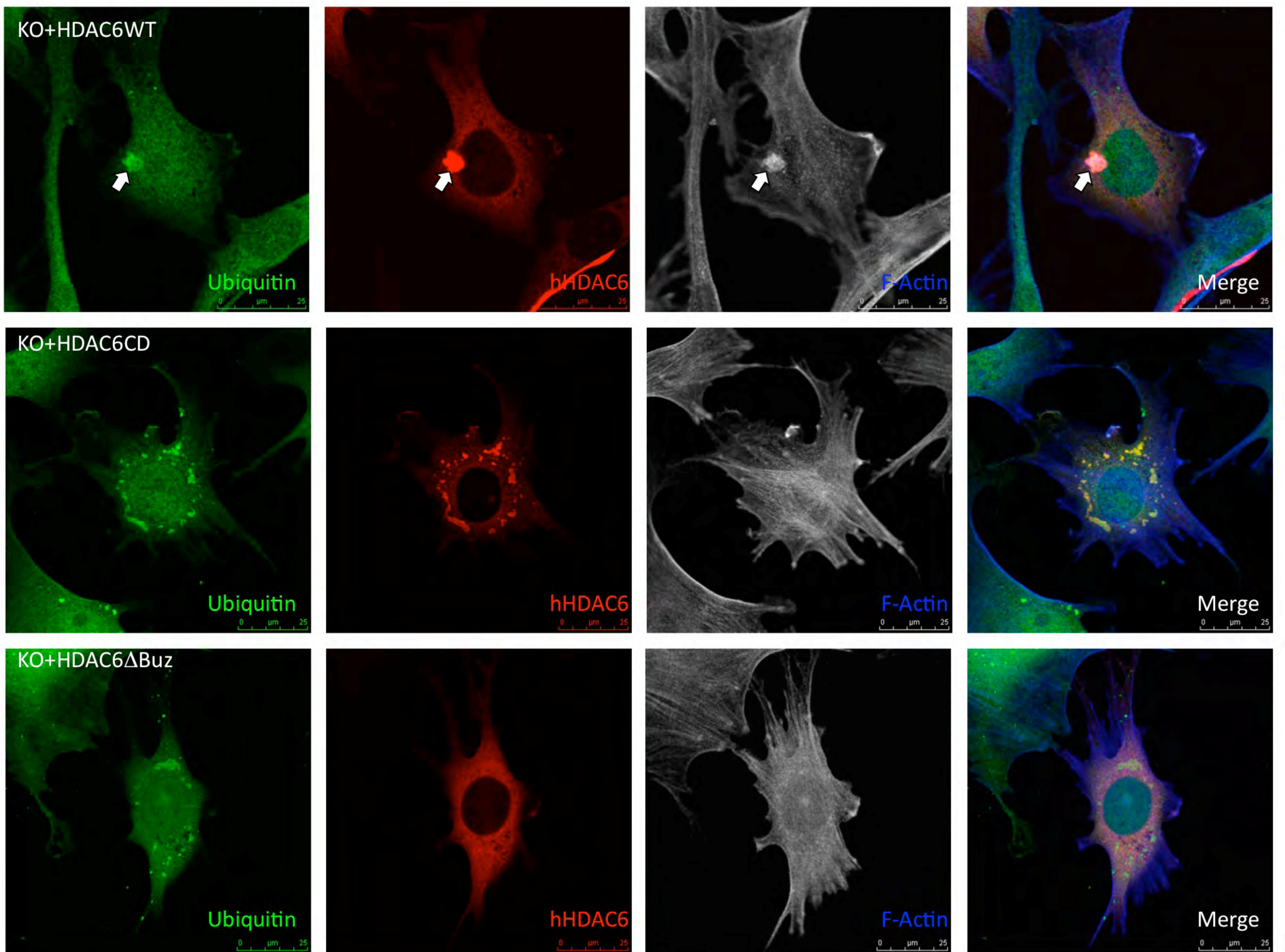
A**B****C**

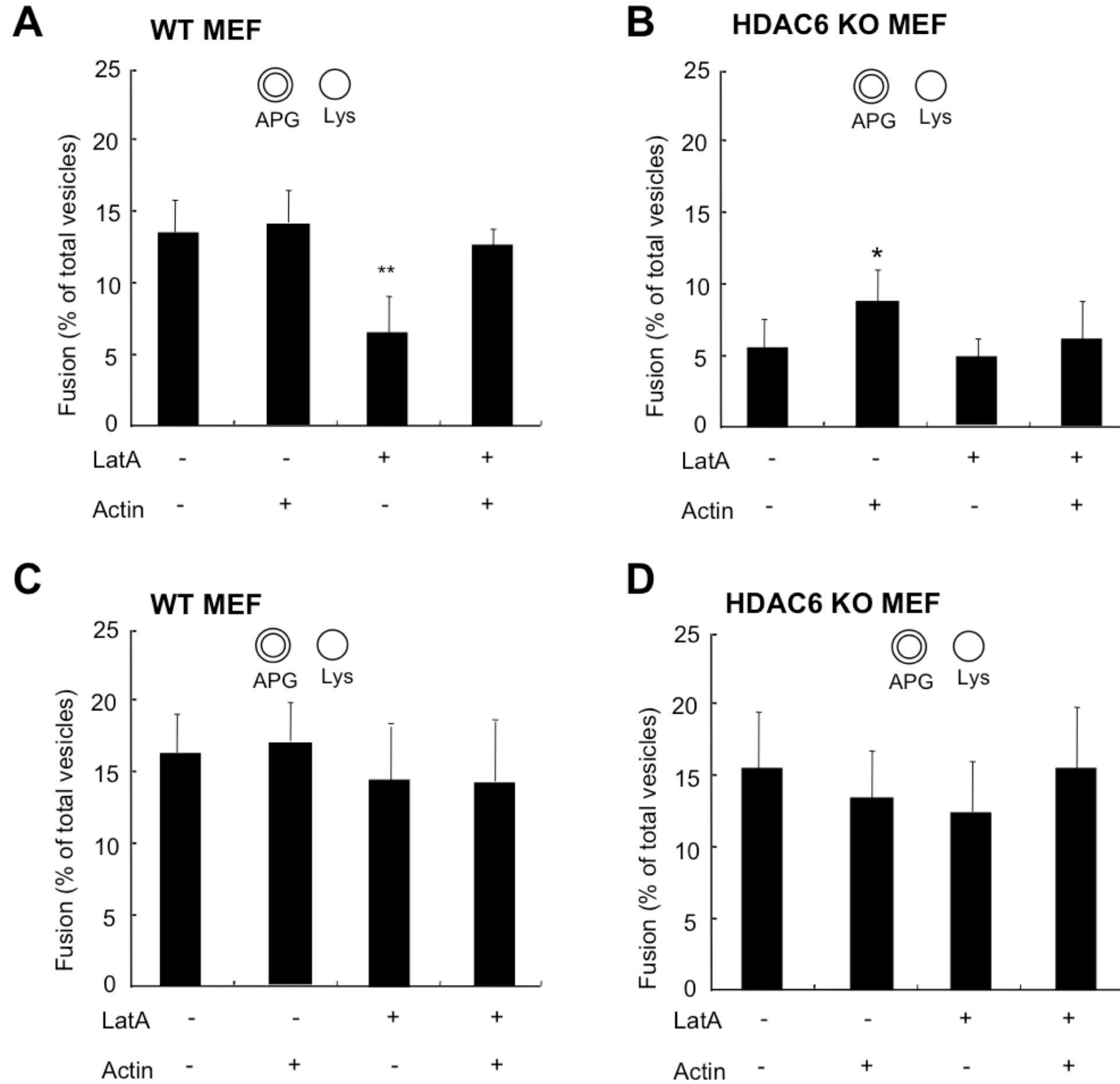
A**B**

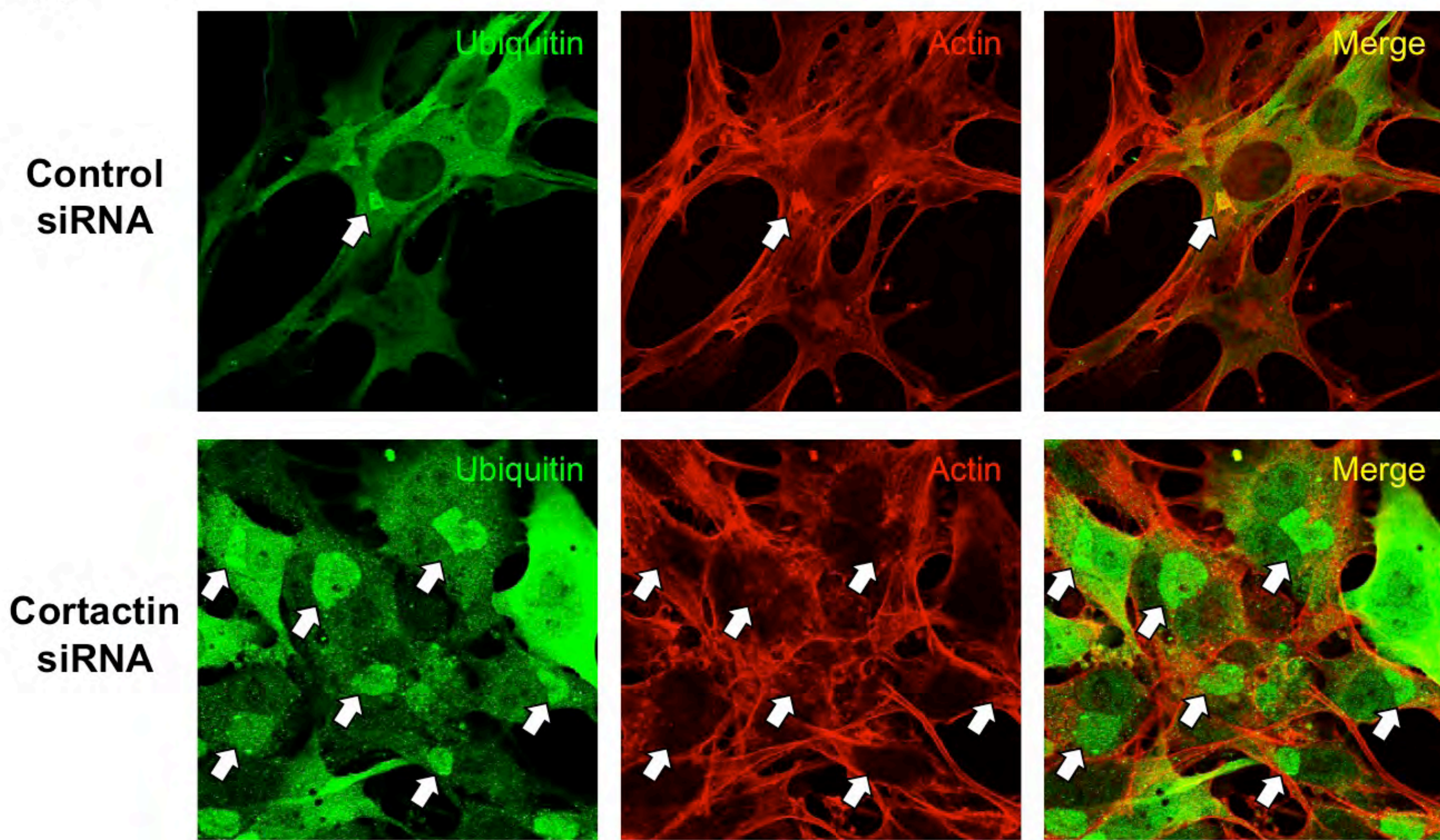
A



B





A**B**